Published in final edited form as:

Cerebellum. 2018 April ; 17(2): 173–190. doi:10.1007/s12311-017-0892-3.

Malformation of the Posterior Cerebellar Vermis Is a Common Neuroanatomical Phenotype of Genetically Engineered Mice on the C57BL/6 Background

Joshua A. Cuoco[1], **Anthony W. Esposito**[1], **Shannon Moriarty**[1], **Ying Tang**[1], **Sonika Seth**[1], **Alyssa R. Toia**[1], **Elias B. Kampton**[1], **Yevgeniy Mayr**[1], **Mussarah Khan**[1], **Mohammad B. Khan**[1], **Brian R. Mullen**[2], **James B. Ackman**[2], **Faez Siddiqi**[3], **John H. Wolfe**[3,4], **Olga V. Savinova**[1], and **Raddy L. Ramos**[1]

[1]Department of Biomedical Sciences, College of Osteopathic Medicine, New York Institute of Technology, Northern Boulevard, PO Box 8000, Old Westbury, NY 11568-8000, USA

[2]Department of Molecular, Cell and Developmental Biology, University of California Santa Cruz, Santa Cruz, CA 95064, USA

[3]Division of Neurology and Research Institute of Children's Hospital of Philadelphia, Philadelphia, PA 19104, USA

[4]Department of Pediatrics, Perelman School of Medicine and W.F. Goodman Center for Comparative Medical Genetics, School of Veterinary Medicine, University of Pennsylvania, Philadelphia, PA, USA

Abstract

C57BL/6 mice exhibit spontaneous cerebellar malformations consisting of heterotopic neurons and glia in the molecular layer of the posterior vermis, indicative of neuronal migration defect during cerebellar development. Recognizing that many genetically engineered (GE) mouse lines are produced from C57BL/6 ES cells or backcrossed to this strain, we performed histological analyses and found that cerebellar heterotopia were a common feature present in the majority of GE lines on this background. Furthermore, we identify GE mouse lines that will be valuable in the study of cerebellar malformations including diverse driver, reporter, and optogenetic lines. Finally, we discuss the implications that these data have on the use of C57BL/6 mice and GE mice on this background in studies of cerebellar development or as models of disease.

Keywords

Transgenic mice; Knock-out mice; C57BL/6; Cerebellar development

Correspondence to: Raddy L. Ramos.

Compliance with Ethical Standards

Conflict of Interest

The authors declare that they have no conflict of interest.

Introduction

The use of mouse models has led to significant advancements in knowledge of cerebellar function and development, as well as cerebellar diseases. Diverse inbred and outbred strains, F1 hybrids, recombinant inbred lines, and consomic strains are among the many powerful mouse tools used by investigators to study the cerebellum. Moreover, a great deal of research devoted to understanding the molecular mechanisms of cerebellar development and disease involves studies using genetically engineered (GE) mice, including transgenic, knock-out, and knock-in lines. In light of novel methods to easily and rapidly manipulate the genome of mice such as the CRISPR Cas system, the production and use of GE mice to model a variety of cerebellar disorders will likely continue to increase in the future.

The background strain of embryonic stem (ES) cells used to produce GE mice as well as the background strain of the mice used to propagate the GE line will affect the observed phenotype. GE mice are often produced using ES cells from FVB/N [1, 2], C57BL/6, and 129/S families of inbred strains—each of which has advantages and limitations. For example, it is known that FVB/N mice are homozygous for mutation of *Pde6B* [3–6], which causes retinal degeneration and blindness within the first month of life. Furthermore, both FVB/N and 129/S inbred strains are homozygous for the deletion polymorphism of *Disc1* [7, 8], which has been implicated in learning and memory in mice [7, 9] as well as schizophrenia in humans [10–12]. Reduced growth or agenesis of the corpus callosum has also been observed in 129/S strains [13]. Finally, C57BL/6 mice are homozygous for a variant of *Cdh23* (cadherin 23; [14]), which results in age-related hearing loss [15] due to dysfunction of cochlear hair-cell tip-links [16, 17].

C57BL/6 mice exhibit spontaneous neurodevelopmental malformations of the posterior cerebellar vermis, which develop postnatally. These malformations are characterized by heterotopia of granule cells in the molecular layer, indicative of neuronal migration defect [18–20]. Several other neuronal and glial cell types are present in cerebellar molecular layer heterotopia (MLH) as well as diverse axonal constituents [21], indicative of abnormal cellular and synaptic organization. Although behavioral and physiological studies linking MLH to functional changes are lacking, the presence of heterotopia in this widely used inbred strain has important implications for its use in studies of the cerebellum.

The mechanisms underlying MLH formation are unknown; however, heterotopia formation is a heritable and weakly penetrant trait requiring homozygosity of one or more C57BL/6 alleles [20]. One predication from earlier findings suggests that MLH should be observed in GE mice either (1) produced with C57BL/6 ES cells or (2) backcrossed to a C57BL/6 background. In a recent report, we did indeed identify GE mice on a C57BL/6 background with heterotopia following analyses of images from the Allen Brain Atlas database [22]. However a limitation of that study was a lack of primary data from histological material prepared and examined in our laboratory. In the present report, primary histology was used to demonstrate that diverse GE mouse lines, including F1 crosses of *Cre*-driver and *loxP*-reporter mice, produce offspring that exhibit heterotopia. In addition, new histological data from the several digital databases provides an extensive list of novel GE mice that exhibit heterotopia, including mice well-suited to study cerebellar development and the MLH

phenotype. Finally, we discuss the implications that these data have on the use of C57BL/6 mice and GE mice on this background in studies of cerebellar development or as models of disease.

Materials and Methods

Approvals for the following studies were obtained from the New York Institute of Technology, University of California Santa Cruz, and the Children's Hospital of Philadelphia. Methods for harvesting brains, tissue sectioning, staining, and identification of heterotopia have been extensively described by our group [19, 20, 22]. In the present report, all brains examined were from mice older than postnatal day (P) 14. Note that we previously determined that MLH are visible as early as P4 and that the presence/absence of heterotopia does not change with age [19]. For this reason, comparisons of heterotopia prevalence between mice of different ages in the present report is appropriate given that all mice were at least 2 weeks old at the time of sacrifice, at which time lobule/fissure patterning and neuronal migration are nearly complete [23]. We previously determined that there are no quantitative differences in the prevalence of cerebellar MLH between sexes [19]; therefore, data from male and female mice are combined. Finally, no differences in heterotopia prevalence have been previously observed between mice obtained directly from commercial vendors and mice bred in an academic vivarium from commercially obtained breeders [19]. All primary histological data from GE lines and crosses were from mice bred in academic vivaria from breeders obtained commercially or unless otherwise specified.

Breeding pairs of B6.Cg-Tg(Tek-cre)1Ywa/J mice (referred to as *Tie2*-Cre mice) were obtained from The Jackson Laboratory; stock #008863; Bar Harbor, ME, where the line was backcrossed onto C57BL/6 mice for ≥ 8 generations and continues to be maintained on a C57BL/6J background. Characterization of this mouse strain has shown panendothelial expression of the *Cre* transgene [24]. Breeding pairs of STOCK-$Hprt^{CAG\text{-}LSL\text{-}ALPL/CAG\text{-}LSL\text{-}ALPL}$ knock-in mice (referred to as $Hprt^{ALPL/ALPL}$ *mice*) were obtained from Dr. Jose Luis Millan (Sanford Burnham Prebys Medical Discovery Center, La Jolla, CA, 92037). This line was developed using ES cells derived from the 129P2/OlaHsd (129Ola) mouse strain as previously described [25] and has been maintained on a C57BL/6 congenic background. $Hprt^{ALPL/ALPL}$ female mice were crossed with *Tie2-Cre*/+ male mice and brains of F1 male mice from these litters were examined for heterotopia regardless of genotype.

Breeding pairs of C57BL/6 J–$Ldlr^{Hlb301}$/J mice (referred to as $Ldlr^{Hlb301/Hlb301}$ mice) were obtained from The Jackson Laboratory where ethylnitrosourea mutagenesis was originally induced in C57BL/6J mice and the line subsequently maintained in this same background [26]. A cohort of *Tie2-Cre*/+ and $Hprt^{ALPL/ALPL}$ mice were each crossed to $Ldlr^{Hlb301\ Hlb301}$ for two generations to obtain a homozygous mutant $Ldlr^{Hlb301/Hlb301}$ background. *Tie2-Cre*/+;$Ldlr^{Hlb301/Hlb301}$ mice were intercrossed with $Hprt^{ALPL/ALPL}$;$Ldlr^{Hlb301/Hlb301}$ mice. Brains from male mice from these litters were examined for the presence of heterotopia regardless of genotype.

Breeding pairs of B6.129P2-*Lyz2*$^{tm1(cre)Ifo}$/J mice (referred to as *Lyz2*^{Cre} mice) were obtained from The Jackson Laboratory (stock #004781). The line was originally produced in 129P2/OlaHsd-derived E14.1 ES cells and backcrossed to C57BL/6J mice for ≥ 6 generations and then maintained on a C57BL/6J background [27]. A cohort of *Lyz2*$^{Cre/+}$ mice were crossed to *Ldlr*^{Hlb301} for two generations to obtain a homozygous mutant *Ldlr*$^{Hlb301/Hlb301}$ background. *Lyz2*$^{Cre/+}$;*Ldlr*$^{Hlb301/Hlb301}$ mice were intercrossed with *Hprt*$^{ALPL/ALPL}$;*Ldlr*$^{Hlb301/Hlb301}$ mice. Brains from male mice from these litters were examined for the presence of heterotopia regardless of genotype.

Breeding pairs of *Isl1*$^{tm1(cre)Sev}$/J driver mice (referred to as *Isl1*^{Cre} mice) were obtained from an existing colony at University of Pennsylvania where they were initially produced using 129S ES cells and backcrossed and maintained on a C57BL/6J background [28]. *Isl1*^{Cre} mice are commercially available (The Jackson Laboratory; stock #024242). Breeding pairs of B6.Cg-Gt(Rosa)26Sor$^{tm14(CAG-tdTomato)Hze}$/J reporter mice (referred to as *Ai14* mice) were purchased from The Jackson Laboratory (stock #007914). *Ai14* mice were produced using 129S6/SvEvTac × C57BL/6, F1-derived G4 ES cells and were subsequently backcrossed and maintained on a C57BL/6J background. *Ai14* mice express tdTomato, a red fluorescent protein, following deletion of a *loxP*-flanked STOP cassette when crossed with mice expressing *Cre* recombinase [29]. A cohort of brains from F1 hybrid mice produced by crossing hemizygous *Isl1*^{Cre} mice and homozygous *Ai14* mice were examined for the presence of heterotopia. In the present report, only F1 hybrid mice that expressed tdTomato were examined for the presence of heterotopia.

Breeding pairs of B6.Cg-Tg(Thy1-GCaMP3)6Gfng mice (referred to as *Thy1-GCaMP3* mice) were purchased from The Jackson Laboratory (stock #029860) where the line was first made using C57BL6/J × CBA F1oocytes and then backcrossed and maintained on a C57BL/6J background. These mice express GCaMP3 in diverse regions of the neo-cortex and subcortical nuclei [30]. These mice were not genotyped; however, only brains that exhibited GCaMP3 expression were used in the present study, signifying that all brains were from mice that were at least hemizygous for the *GCaMP3* allele.

Breeding pairs of B6.*Cg-Snap25*$^{tm3.1Hze}$/J mice (referred to as *Snap25*^{GCaMP6s}mice) were purchased from The Jackson Laboratory (stock #025111) where the line was produced using 129S6/SvEvTac × C57BL/6 F1-derived G4 ES cells and then backcrossed and maintained on a C57BL/6J background. These mice express GCaMP6s exclusively in neurons throughout the brain. These mice were not genotyped; however, only brains that exhibited GCaMP6s expression were used in the present study, signifying that all brains were from mice that were at least hemizygous for the *GCaMP6s* allele.

Breeding pairs of C57BL/6J - Tg (Thy1 -GCaMP6s)GP4.3Dkim/J mice (referred to *Thy1-GCaMP6s* mice) were purchased from The Jackson Laboratory (stock #024275). This line was created and has been maintained on a C57BL/6J background. These mice were not genotyped; however, only brains that exhibited GCaMP6s expression were used in the present study, signifying that all brains were from mice that were at least hemizygous for the *GCaMP6s* allele.

Brains from a cohort of Tg(CAG-EGFP/Map1lc3b)53Nmz mice [31] (referred to as *LC3-eGFP* mice) were backcrossed and maintained on a C57BL/6 background in a colony at New York Institute of Technology College of Osteopathic Medicine. Brains were generously donated by Qiangrong Liang. These mice were not genotyped; however, only brains that exhibited *eGFP* expression were used in the present study, signifying that all brains were from mice that were at least hemizygous for the *eGFP* allele.

Examination of Digital Histological Material

We have extensively described our approach of using digital histological data found in the Allen Brain Atlas (ABA; brain-map.org) as a tool to identify the ontogeny, cell types, axonal constituents, and gene expression profiles of cerebellar [19–22] and neocortical heterotopia [32, 33]. In the present report, we specifically used data from the *Mouse Connectivity* database, which includes histology from neuronal tracing experiments performed in C57BL/6J mice as well as in diverse *Cre*-driver lines [34–36]. Additional material was examined from the *Transgenic Characterization* database, which contains in situ *hybridization* data from expression studies performed on numerous driver lines (*Cre, Dre, Flp*, etc.) and reporter lines (*loxP, FRT*, etc) in addition to driver-reporter hybrid mice as previously described [29, 37–39]. Approximately 8–12 photomicrographs of the posterior cerebellum from each brain in these datasets were examined. Brains containing MLH were documented and digital photomicrographs of representative examples were archived and annotated. Note that in the present report, we use the abbreviated mouse nomenclature for driver and reporter lines found on the ABA webpages when discussing these data below so that readers can more easily find these same data online. However, in Tables 1 and 2, we provide the official strain names for all lines specifically described in the text. Additional information about the driver and reporter lines can be found at the following page on the ABA website (http://help.brain-map.org/display/mouseconnectivity/Documentation).

Virtual histological material was also examined from the *Cell Type Specific Connectivity* database and the *Transgenic: Cell Counts* database of the Mouse Brain Architecture Project (MBAP; http://mouse.brainarchitecture. org/cellcounts/hua/), the Enhancer TRAP mouse line database (eTRAP; https://enhancertrap.bio.brandeis.edu/), and the GENSAT Cre Mice database (http://www.gensat.org/cre.jsp) according to search methods previously described [40]. A description of the methods used in the preparation of data in the MBAP database can be found at the following website: http://www.brainarchitecture.org/documentation. Methods used in the preparation of data in the GENSAT Cre database [41–43] and eTRAP database [44] have been previously described. Brains exhibiting MLH were documented and digital photomicrographs of representative examples were archived and annotated. Note that in the present report, we use the abbreviated mouse nomenclature for driver and reporter lines found on the MBAP databases when discussing these data in the text below so that readers can more easily find these same data online. However, in Table 3, we provide the official strain names for all lines described in the text.

Results

Heterotopia Are Found in GE Driver and Reporter Mice as well as Driver-Reporter Crosses

In the time since our previous report documenting cerebellar heterotopia in GE mice [22], vast amounts of new data have been added to the *Mouse Connectivity* and *Transgenic Characterization* databases of the ABA. In light of this, we performed analyses of this additional histological data in order to identify the potential presence of heterotopia in novel GE mouse lines. A total of 1702 serial-sectioned brains from the *Mouse Connectivity* database were examined for the presence of cerebellar MLH using methods previously described by our group and which have been successful in identifying cerebellar MLH [19–22]. Material in this database includes > 120 coronal sections throughout the entire rostral-caudal extent of each brain from 101 distinct *Cre*-driver mice injected with neuronal tracers for the study of the mouse connectome [35]. Material from wild-type C57BL/6J mice injected with neuronal tracers is also found in this database. We have extensively documented that MLH are readily identifiable in coronal and sagittal sections by identification of several histological features characteristically found at the vermal midline. For example, compared to the normal cyctoarchitecture of the posterior vermis (Fig. 1a–b), MLH are characterized by heterotopic collections of stained cells that are present in between the molecular layers of lobules VIII and IX (Fig. 1c–d) which can be seen as forming an “island” of cells surrounded by an otherwise normal appearing molecular layer. As shown in Fig. 1e–f, heterotopia can also be characterized by a bridge of stained cells traversing the molecular layers of lobules VIII and IX. In both brains with heterotopia, regions lacking pia are evident between lobules VIII and IX in those areas containing heterotopic granule cells that have failed to migrate.

MLH were indeed apparent in brains found in the *Mouse Connectivity* database. We observed MLH in 920 of 1702 (54%) brains in this database which included 91 of 101 (90%) distinct *Cre*-driver lines that exhibited heterotopia. A list of *Cre*-driver lines exhibiting heterotopia is found in Table 1, including the number of mice in each line that exhibited heterotopia as well as a representative reference experiment identification number which can be used to view this material directly on the ABA website. Using this approach, our analyses of heterotopia prevalence cannot rule *out* that MLH may be found in a given *Cre*-driver line, when $n = 0$ heterotopia are observed from among a small sample of brains. Instead, this type of analysis can provide evidence that a given mouse line does exhibit some prevalence of MLH, when $n \geq 1$ cases with heterotopia is identified. For example, as indicated in Table 1, we did not find any brains with heterotopia among 10 of 101 *Cre*-driver lines. However, with only one exception, fewer than eight total brains were available for examination from each of these driver lines that did not demonstrate any prevalence of heterotopia. Nevertheless, as shown in Table 1, we did identify heterotopia in over 90 distinct *Cre*-driver lines even when very few brains were available for examination for that line.

Figure 2 illustrates examples of the normal cytoarchitecture of the posterior vermis (a–c) and MLH (d–f) in a C57BL/6 mouse brain found in the *Mouse Connectivity* database. As shown in Fig. 2(g–i), MLH observed in *Cre*-driver lines in this database had cytoarchitecture and

histological profiles identical to heterotopia observed in C57BL/6 mice (Fig. 2d–f) [19, 20]. As indicated in Table 1, we found that all but 3 of 91 *Cre*-driver lines exhibiting MLH were maintained on a congenic C57BL6/J background. Grm2-Cre_MR90 and Oxtr-Cre_ON66 mice (see Table 1 for details of each mouse line) were reported to be on a FVB/NCrl:CD1(ICR) background while the background of Lypd6-Cre_KL156 was not reported (official mouse line name was not found). As shown in Table 1, only four of ten lines not exhibiting MLH were on a congenic C57BL6/J background, while the remaining six where either on an unknown or FVB/NCrl:CD1(ICR) background.

Although not a specific goal of the present study, we observed GFP-labeled axons in heterotopia in C57BL/6J wild-type mice Fig. 2(d–f) as well as *Cre*-driver lines in the *Mouse Connectivity* database which differed from the normal pattern of GFP-labeled axons restricted to the granule cell layer observed in mice without heterotopia (Fig. 2a–c). For example, as shown in Fig. 2(g–i), GFP axons with swellings characteristic of *en passant* synapses were visible among heterotopic granule cells in a Crh - IRES - Cre (BL) mouse (experiement:167213641; Table 1) which was injected with a *Cre*-dependent virus targeting the dorsal cochlear nucleus. GFP-labeled axons in heterotopia were also observed in a Slc6a4-CreERT2_EZ13 mouse (experiment #114155190; Table 1), a Rasgrf2–2A-dCre mouse (experiment #313141786; Table 1), and a Sim1-Cre mouse (experiment:165035106; Table 1) which were injected with a *Cre*-dependent virus targeting the dorsal raphe nucleus, parabrachial nucleus, and lateral hypothalamic area, respectively. Taken together, these data point to widespread prevalence of MLH in *Cre*-driver lines and suggest that diverse axon-types from various subcortical nuclei innervate cells in heterotopia.

Recognizing that C57BL/6 mice and numerous *Cre*-driver lines exhibit MLH, we predicted that reporter lines would also exhibit heterotopia. Therefore, an examination of data from the *Transgenic Characterization* of the ABA database was performed with specific focus on all available data from reporter lines. Figure 3 illustrates examples of the normal cytoarchitecture of the posterior vermis (a–b) and MLH (c–d, e–f) in sagittal sections of C57BL/6 mouse brains found in this database. As shown in Fig. 3(g–j) and Table 1, we did indeed observe MLH in several reporter lines including: *Ai14*, *Ai27*, *Ai32* (data not shown), *Ai39*, and *Ai75*(data not shown)mice(see Table 1 fordetailsabout each reportermouse line).The cytoarchitecture and histological profiles of MLH in these reporter lines were identical to heterotopia observed in C57BL/6 mice (Fig. 3c–f) and are consistent with our observations of MLH in *Cre*-driver lines. As shown in Table 1, all reporter lines found to exhibit heterotopia were maintained on a congenic C57BL/6 background. When crossed to *Cre*-driver lines, these reporter lines can be used to express variants of the optogenetic proteins channelrhodopsin (*Ai27*, *Ai32*) or halorhodopsin (*Ai39*). These data demonstrate that *Cre*-driver lines as well as reporter lines can exhibit cerebellar heterotopia.

A major experimental use of the aforementioned GE lines includes producing driver-reporter crosses for selective labeling and manipulation of particular cell types. Consequently, we examined novel data on the *Transgenic Characterization* database of driver-reporter F1 hybrids for the presence of heterotopia. Table 2 lists examples of MLH observed in diverse F1 hybrids including those resulting in expression of a variety of fluorescent proteins, genetically encoded calcium indicators, and optical stimulators/inhibitors. In all cases, both

the driver line (Table 1) and the reporter line were on a congenic C57BL/6 background. Figure 4 illustrates that F1 crosses of the same driver line known to exhibit heterotopia with several different reporter lines (ex. *Ai32, Ai35, Ai40, Ai57, Ai87*; see Table 2 for details of each line) can result in offspring that exhibit heterotopia. These data indicate that heterotopia formation is a heritable trait that can be observed in diverse crosses of GE mice.

Additional Datasets Demonstrating Cerebellar Heterotopia in GE Mice

In order to confirm and extend on our observations of heterotopia in GE mice in the ABA, we searched for additional databases with histological data from GE mice including the MBAP, eTRAP, and GENSAT Cre databases. As shown in Fig. 5 and Table 3, heterotopia were evident in diverse *Cre* lines and driver/reporter crosses present in the MBAP databases. In particular, we observed heterotopia in 8 out of 20 (40%) distinct driver/reporter F1 hybrid lines (17 of 151 total brains examined had heterotopia) in the MBAP databases including *Cre*-driver lines crossed with different reporter lines. We also observed heterotopia in two out of two *Cre*-driver mouse lines (five out of ten brains examined) found in the *Cell Type Specific Connectivity* database of the MBAP. As shown in Table 3, all *Cre*-driver lines and the and crosses with *Ai14* reporter mice identified in the MBAP databases are the same lines and identical crosses found to exhibit heterotopia in our analysis of data in the ABA databases. We list representative examples of similar findings in both the MBAP and ABA databases in Table 3. These results confirm our observations of MLH in GE mice using data from independent research groups.

A total of 140 distinct mouse lines were found in eTRAP database though only one to two brains per line were available for examination. These lines were developed and maintained on a C57BL/6 background [44]. Heterotopia were observed in 9 of 140 (6.43%) lines in the eTRAP database (including lines: PBAS, P222, P181, P133, P126, P103, P125, P074, P024). As shown in Fig. 5(j–o), heterotopia in mice found in the eTRAP database were identical to those observed in C57BL/6 mice as well as other GE lines on this background.

We did not find any brains with heterotopia among the 145 different *Cre* lines present in the GENSET database, as these mice were generated on a FVB/N background. Nevertheless, our observations in the MBAP and eTRAP databases extend upon our observations in the ABA databases.

Examination of Primary Histological Data Confirm Findings Using Databases

In order to confirm and extend on our observations using digital databases, we examined primary histological material prepared in our laboratory from a variety of GE mice for the presence of heterotopia. All of the lines in these studies were bred in academic vivaria and were maintained on a C57BL/6 background. First, as shown in Fig. 3(k–l), heterotopia were found in two of four (50%) *Ai14* reporter mouse brains examined, which is consistent with our observations of heterotopia in crosses with *Ai14* mice in the ABA and MBAP databases (Tables 2 and 3). In addition, we observed heterotopia in two of four (50%) *Tie2-Cre*/+ mice, three of six (50%) $Lyz2^{Cre/+}$ mice, and five of eight (62.5%) $Ldlr^{Hlb301/Hlb301}$ mice (data not shown). However, we did not observe heterotopia in any $Hprt^{ALPL/ALPL}$ mice ($n = 6$; data not shown).

Brains from several different F1 driver-reporter crosses were also examined in our laboratory. For example, we observed heterotopia in 6 of 16 brains (35.7%) from *Isl1*$^{Cre/+}$; *Ai14* mice (Fig. 6g–l). As shown in the representative examples in Fig. 6, robust tdTomato-expression was observed in scattered granule cells and mossy fibers in the posterior cerebellum in *Isl1*$^{Cre/+}$; *Ai14* mice. MLH in these F1 hybrid mice had heterotopia identical to that observed in C57BL/6 mice or other *Cre*-driver mice crossed to *Ai14* mice. As shown in Fig. 6(k–l), tdTomato-labeled granule cells as well as mossy fiber axons were present in heterotopia though the exact origin of these axonal projections is unknown.

As shown in Fig. 7(c–d), we observed heterotopia in *Tie2-Cre/+;Hprt*$^{ALPL/+}$ F1 mice (6 of 19 brains; 31.57%). Heterotopia were also present in 4 out of 17 (23.5%) mice produce by crossing *Tie2-Cre/+;Ldlr*$^{Hlb301/Hlb301}$ mice with *Hprt ALPL/ALPL;LdlrHlb301/Hlb301* mice. Heterotopia were also present in 4 out of 14 (28.6%) mice produced by crossing *Lyz2C re / +; Ldlr*$^{Hlb301/Hlb301}$ mice with *Hprt* $^{ALPL / ALPL}$*;Ldlr*$^{Hlb301/Hlb301}$ mice. As shown in Fig. 7(g–h), heterotopia were also found in the progeny of three-way crosses of GE mice in the Allen Brain Atlas. Thus, primary histological analyses in our laboratory confirm that crosses of driver and reporter mice can result in progeny that exhibit heterotopia. Additionally, we identify *Isl1*^{Cre} mice as a novel resource to for labeling granule cells and mossy fibers in heterotopia.

A major goal of the present study was to identify mouse lines that would be valuable for the study of cerebellar heterotopia. As shown in Fig. 8 from primary histological data produced in our laboratory, several additional GE mouse lines (all on a congenic C57BL/6 background) exhibit heterotopia and can be used for calcium imaging of GCaMP variants. For example, *Thy1-GCaMP3*/+ mice with heterotopia (Fig. 8a–c; 3 of 12 brains; 25%) allow for imaging of labeled axons in heterotopia which likely include spino-cerebellar and reticulo-cerebellar projections. *Thy1-GCaMP6s*/+ mice with heterotopia (Fig. 3d–f; three of nine brains; 33%) are well-suited for imaging the few scattered GCaMP6s-expressing cells found in heterotopia and in the normal granule cell layer. In contrast, lack of clear GCaMP6s expression in the cerebellum makes *Snap25*$^{GCaMP6s/+}$ mice (Fig. 8g–i) not very useful as a tool for calcium imaging in mice with heterotopia (three of six brains; 50%). Finally, as shown in Fig. 8(j–l), GFP expression in the somata and dendrites of *LC3-eGFP* mice with heterotopia (5 of 13 brains with heterotopia; 38.46%) allow for determination of changes in Purkinje cell development and morphology associated with heterotopia formation.

Discussion

Cerebellar Heterotopia Are Commonly Found in GE Mice

In the present report, we demonstrate that malformation of the posterior cerebellar vermis is a common phenotype of GE mice on the C57BL/6 background. In particular, heterotopia were observed in numerous *Cre*-driver mice, reporter mice, and several other GE mice. Moreover, crossing driver and reporter mice also resulted in progeny that exhibit heterotopia. An important caveat to our approach is that we can only identify GE lines that exhibit the phenotype when at least one brain was observed with a malformation from a sample of brains from a given GE line. In contrast, this approach cannot rule out that a line does exhibit some prevalence of heterotopia when we do not observe any heterotopia in a sample

of brains examined from any given line. Furthermore, it cannot be assumed that if heterotopia are not observed in a small sample of brains from one or more lines that are intended to be crossed that F1 progeny from these strains will not exhibit heterotopia. Our findings exemplify this point. Specifically, we did not observe heterotopia0 of 6 $Hprt^{ALPL/ALPL}$ mice; however, we did find heterotopia in *Tie2-Cre/+;*$Hprt^{ALPL/+}$ F1 mice.

Another caveat to our approach of using digital histological databases is that it relies heavily on the number of brains available to examine, the number of sections available per brain, the quality of sectioning and staining, etc. which may have affected our findings of different percentages of GE lines with heterotopia among the different databases that were used. Thus, there are likely more lines that exhibit heterotopia that what was observed, and there also exists the possibility that all GE lines on a C57BL/6 background will exhibit cerebellar heterotopia with some prevalence.

Our findings extend on our earlier observations of heterotopia in C57BL/6 mice and related strains [19–22] and suggest that heterotopia are caused by a heritable, weakly penetrant recessive allele found in the C57BL/6 lineage [20]. Consistent with this model, nearly all of the GE mice found to exhibit heterotopia were either created with C57BL/6 ES cells or were backcrossed onto the C57BL/6 background. Furthermore, we did not observe any heterotopia in the GENSAT *Cre* database, which includes data from *Cre* lines generated from ova of FVB/N mice (Taconic Farms), a strain that we previously found to never exhibit heterotopia [20]. One prediction from our findings is that some prevalence of heterotopia will be present in any GE line or hybrid cross of GE lines once homozygosity for the C57BL/6 heterotopia allele is present in line. Likewise, it is anticipated that no heterotopia will be observed in F1 hybrid mice produced by crossing one GE line on a C57BL/6 background with another GE line on a different background (such as 129 or DBA; [20]). Thus, identifying the causal allele for heterotopia formation is an important area for future research.

Implications of Heterotopia on the Use of GE Mice

Our results have important and broad implications for the use of GE mice in studies of cerebellar development, function, and disease. First, data in the present report argue strongly that some prevalence of heterotopia formation will be found in most (if not all) GE mice produced with C57BL/6 ES cells or backcrossed onto the C57BL/6 background. Thus, investigators will have to consider how the presence of heterotopia in experimental and control groups will affect interpretation of study outcomes. For example, knock-out mice are a popular tool for examining the role of a given gene and gene product on cerebellar development. Likewise, *Cre*-driver lines are commonly crossed with “floxed” lines to produce conditional knock-in or knock-out lines for similar types of studies. One prediction from our results is that a majority of GE mouse models will exhibit heterotopia with some prevalence simply due to the contribution of the C57BL/6 background. In this scenario, GE mice exhibiting heterotopia could be interpreted as arising due to genetic perturbation. Thus, careful histological examination of hetero/hemizygous and homozygous mice (and wild-type controls) will be necessary to evaluate results in developmental studies using GE mice on a C57BL/6 background.

Despite the above caveats, developmental studies using GE mice have the potential to contribute to understanding of the molecular mechanisms of heterotopia formation. For example, consider the scenario where a knock-out or conditional knockout line exhibits 100% prevalence of MLH formation, while the hemizygous mice exhibit a prevalence of ~ 30% (similar to C57BL/6 wild-type controls). Conversely, consider the scenario where the knock-out or conditional knock-out exhibits 0% prevalence of MLH formation, while the hemizygous mice exhibit a prevalence of ~ 30% (similar to wild-type controls). Both of these disparate findings would strongly point to an interaction between a causal allele for heterotopia formation with the gene deleted in the GE model.

Resources for Studying Development and Malformation of the Posterior Cerebellum

In the present report, we identify numerous GE models that are well-suited for the study of the formation and physiological consequences of heterotopia. For example, we have identified that *Isl1*^{Cre} mice as well as Gabra6-IRES-Cre, Kcnc2-Cre, and Calb1–2A-dgCre lines from the ABA exhibit heterotopia (Table 1). Given that impairment of granule cell migration is the characteristic feature of MLH, and that Isl1 and Gabra6 are only expressed in granule cells [45, 46], *Isl1*^{Cre} and Gabra6-IRES-Cre lines (Table 1) will be valuable models for future use in live-imaging and/or gene expression studies when crossed to reporter mice which also exhibit some prevalence of MLH. Similarly, *LC3-eGFP* as well as Kcnc2-Cre and Calb1–2A-dgCre lines will be valuable for targeting Purkinje cells associated with heterotopia. Thus, combined with our findings of MLH in GCaMP mice (*Thy1-GCAMP3* and *Thy1-GCAMP6s* lines) and channelrhodopsin mouse lines, we demonstrate that there are diverse GE mice that will be valuable in future physiological, developmental, and mechanistic studies

Genetic and Cellular Model of Heterotopia Formation in C57BL/6 Mice and GE Mice on the C57BL/6 Background

Several recent findings strongly suggest that heterotopia formation is a trait controlled by one or more weakly penetrant recessive alleles [20]. First, F1 hybrid crosses between C57BL/6 and DBA/2J mice never exhibit heterotopia. Crosses between C57BL/6 and 129S6 mice also do not exhibit heterotopia, suggesting that homozygosity of one or more C57BL/6 alleles is required for heterotopia formation. Second, recombinant inbred mice such as the BXD29-Tlr4^{lps-2J}/J line (where C57BL/6 and DBA/2J are parental strains) also exhibit heterotopia, consistent with a requirement of homozygosity for heterotopia expression. Finally, consomic mice with chromosome 1 from the A/J mouse genotype on an otherwise C57BL/6 background also exhibit heterotopia, suggesting that one or more causal allele is found outside of chromosome 1.

While the genetic mechanisms are still unknown, the cellular and tissue-level mechanisms of heterotopia formation are becoming better understood. In particular, histological analyses clearly demonstrate a loss of pia in regions containing heterotopic granule cells. In addition, heterotopia are also associated with spatial and morphological disorganization of Bergmann glia and radial fibers [19]. Thus, we posit that a deficit in pia formation during cerebellar foliation likely affects radial glial endfoot attachment and the formation of the glial limitans. Alternatively, abnormal development of Bergmann glial fibers affects pial formation. In

either case, disruption of radial fibers ultimately leads to the failure of granule cells to exit the molecular layer (external granule cell layer) which leads to heterotopia formation by these cells. Lending further support to our model of heterotopia formation, knock-out mice with deletion of molecules affecting leptomeningeal or radial glia integrity such as b1-integrin [47], γ3-laminin [48], and dystroglycan [49, 50] display heterotopia that are nearly identical (but more severe) to those observed in C57BL/6 mice and GE mice on the C57BL/6 background.

Conclusion

Malformation of the posterior cerebellar vermis is a common neuroanatomical phenotype of genetically engineered mice on the C57BL/6 background and should be considered when designing studies using mouse models on this background.

Acknowledgments

Funding information Supported in part by NIH grant R01-NS088667 (JHW); FS was supported in part by NIH training grant T32-NS007413.

References

1. Auerbach AB, Norinsky R, Ho W, Losos K, Guo Q, Chatterjee S, et al. No title. Transgenic Res. 2003;12:59–69. [PubMed: 12650525]
2. Taketo M, Schroeder AC, Mobraaten LE, Gunning KB, Hanten G, Fox RR, et al. FVB/N: an inbred mouse strain preferable for transgenic analyses. Proc Natl Acad Sci USA. 1991;88:2065–9. [PubMed: 1848692]
3. Bowes C, Li T, Danciger M, Baxter LC, Applebury ML, Farber DB. Retinal degeneration in the rd mouse is caused by a defect in the beta subunit of rod cGMP-phosphodiesterase. Nature. 1990;347:677–80. [PubMed: 1977087]
4. Bowes C, Li T, Frankel WN, Danciger M, Coffin JM, Applebury ML, et al. Localization of a retroviral element within the rd gene coding for the beta subunit of cGMP phosphodiesterase. Proc Natl Acad Sci USA. 1993;90:2955–9. [PubMed: 8385352]
5. Caley DW, Johnson C, Liebelt RA. The postnatal development of the retina in the normal and rodless CBA mouse: a light and electron microscopic study. Am J Anat. 1972;133:179–212. [PubMed: 5009246]
6. Pittler SJ, Baehr W. Identification of a nonsense mutation in the rod photoreceptor cGMP phosphodiesterase beta-subunit gene of the rd mouse. Proc Natl Acad Sci USA. 1991;88:8322–6. [PubMed: 1656438]
7. Koike H, Arguello PA, Kvajo M, Karayiorgou M, Gogos JA. Disc1 is mutated in the 129S6/SvEv strain and modulates working memory in mice. Proc Natl Acad Sci USA. 2006;103:3693–7. [PubMed: 16484369]
8. Clapcote SJ. Deletion polymorphism of Disc1 is common to all 129 mouse substrains: implications for gene-targeting studies of brain function. Genetics. 2006;173:2407–10. [PubMed: 16751659]
9. Kuroda K, Yamada S, Tanaka M, Iizuka M, Yano H, Mori D, et al. Behavioral alterations associated with targeted disruption of exons 2 and 3 of the Disc1 gene in the mouse. Hum Mol Genet. 2011;20: 4666–83. [PubMed: 21903668]
10. Ekelund J, Hennah W, Hiekkalinna T, Parker A, Meyer J, Lönnqvist J, et al. Replication of 1q42 linkage in Finnish schizophrenia pedigrees. Mol Psychiatry. 2004;9:1037–41. [PubMed: 15197400]
11. Cannon TD, Hennah W, van Erp TGM, Thompson PM, Lonnqvist J, Huttunen M, et al. Association of DISC1/TRAX haplotypes with schizophrenia, reduced prefrontal gray matter, and

impaired short-and long-term memory. Arch Gen Psychiatry. 2005;62:1205–13. [PubMed: 16275808]

12. Callicott JH, Straub RE, Pezawas L, Egan MF, Mattay VS, Hariri AR, et al. Variation in DISC1 affects hippocampal structure and function and increases risk for schizophrenia. Proc Natl Acad Sci USA. 2005;102:8627–32. [PubMed: 15939883]
13. Wahlsten D, Metten P, Crabbe JC. Survey of 21 inbred mouse strains in two laboratories reveals that BTBR T/+ tf/tf has severely reduced hippocampal commissure and absent corpus callosum. Brain Res. 2003;971:47–54. [PubMed: 12691836]
14. Noben-Trauth K, Zheng QY, Johnson KR. Association of cadherin 23 with polygenic inheritance and genetic modification of sensori-neural hearing loss. Nat Genet. 2003;35:21–3.
15. Kane KL, Longo-Guess CM, Gagnon LH, Ding D, Salvi RJ, Johnson KR. Genetic background effects on age-related hearing loss associated with Cdh23 variants in mice. Hear Res. 2012;283:80–8. [PubMed: 22138310]
16. Johnson KR, Yu H, Ding D, Jiang H, Gagnon LH, Salvi RJ. Separate and combined effects of Sod1 and Cdh23 mutations on age-related hearing loss and cochlear pathology in C57BL/6J mice. Hear Res. 2010;268:85–92. [PubMed: 20470874]
17. Sotomayor M, Weihofen WA, Gaudet R, Corey DP. Structural determinants of cadherin-23 function in hearing and deafness. Neuron. 2010;66:85–100. [PubMed: 20399731]
18. Tanaka M, Marunouchi T. Abnormality in the cerebellar folial pattern of C57BL/6J mice. Neurosci Lett. 2005;390:182–6. [PubMed: 16139954]
19. Mangaru Z, Salem E, Sherman M, Van Dine SE, Bhambri A, Brumberg JC, et al. Neuronal migration defect of the developing cerebellar vermis in substrains of C57BL/6 mice: cytoarchitecture and prevalence of molecular layer heterotopia. Dev Neurosci. 2013;35:28–39. [PubMed: 23428637]
20. Van Dine SE, Siu NY, Toia A, Cuoco JA, Betz AJ, Bolivar VJ, et al. Spontaneous malformations of the cerebellar vermis: prevalence, inheritance, and relationship to lobule/fissure organization in the C57BL/6 lineage. Neuroscience. 2015;310:242–51. [PubMed: 26383253]
21. Van Dine SE, Salem E, Patel DB, George E, Ramos RL. Axonal anatomy of molecular layer heterotopia of the cerebellar vermis. J Chem Neuroanat. 2013;47:90–5. [PubMed: 23261868]
22. Ramos RL, Van Dine SE, George E, Patel D, Hoplight BJ, Leheste JR, et al. Molecular layer heterotopia of the cerebellar vermis in mutant and transgenic mouse models on a C57BL/6 background. Brain Res Bull. 2013;97:63–8. [PubMed: 23735805]
23. Sudarov A, Joyner AL. Cerebellum morphogenesis: the foliation pattern is orchestrated by multi-cellular anchoring centers. Neural Dev. 2007;2:26. [PubMed: 18053187]
24. Kisanuki YY, Hammer RE, Miyazaki J, Williams SC, Richardson JA, YanagisawaM.Tie2-Cre transgenic mice: anew modelfor endothelial cell-lineage analysis in vivo. Dev Biol. 2001;230:230–42. [PubMed: 11161575]
25. Sheen CR, Kuss P, Narisawa S, Yadav MC, Nigro J, Wang W, et al. Pathophysiological role of vascular smooth muscle alkaline phosphatase in medial artery calcification. J Bone Miner Res. 2015;30: 824–36. [PubMed: 25428889]
26. Svenson KL, Ahituv N, Durgin RS, Savage H, Magnani PA, Foreman O, et al. A new mouse mutant for the LDL receptor identified using ENU mutagenesis. J Lipid Res. 2008;49:2452–62. [PubMed: 18632552]
27. Clausen BE, Burkhardt C, Reith W, Renkawitz R, Förster I. Conditional gene targeting in macrophages and granulocytes using LysMcre mice. Transgenic Res. 1999;8:265–77. [PubMed: 10621974]
28. Yang L, Cai C- L, Lin L, Qyang Y, Chung C, Monteiro RM, et al. Isl1Cre reveals a common Bmp pathway in heart and limb development. Development. 2006;133:1575–85. [PubMed: 16556916]
29. Madisen L, Zwingman TA, Sunkin SM, SW O, Zariwala HA, Gu H, et al. A robust and high-throughput Cre reporting and characterization system for the whole mouse brain. Nat Neurosci. 2010;13: 133–40. [PubMed: 20023653]
30. Chen Q, Cichon J, Wang W, Qiu L. Lee S-JR, Campbell NR, et al. imaging neural activity using Thy1-GCaMP transgenic mice. Neuron. 2012;76:297–308. [PubMed: 23083733]

31. Mizushima N, Yamamoto A, Matsui M, Yoshimori T, Ohsumi Y. In vivo analysis of autophagy in response to nutrient starvation using transgenic mice expressing a fluorescent autophagosome marker. Mol Biol Cell. 2004;15:1101–11. [PubMed: 14699058]
32. Ramos RL, Smith PT, DeCola C, Tam D, Corzo O, Brumberg JC. Cytoarchitecture and transcriptional profiles of neocortical malformations in inbred mice. Cereb Cortex. 2008;18:2614–28. [PubMed: 18308707]
33. Ramos RL, Siu NY, Brunken WJ, Yee KT, Gabel LA, Van Dine SEHB. Cellular and axonal constituents of neocortical molecular layer heterotopia. Dev Neurosci. 2014;36:477–89. [PubMed: 25247689]
34. Harris JA, Oh SW, Zeng H. Adeno-associated viral vectors for anterograde axonal tracing with fluorescent proteins in nontransgenic and cre driver mice. Curr. Protoc. Neurosci 2012;Chapter 1:Unit 1.20:1–18.
35. SW O, Harris JA, Ng L, Winslow B, Cain N, Mihalas S, et al. A mesoscale connectome of the mouse brain. Nature. 2014;508:207–14. [PubMed: 24695228]
36. Kuan L, Li Y, Lau C, Feng D, Bernard A, Sunkin SM, et al. Neuroinformatics of the Allen Mouse Brain Connectivity Atlas. Methods. 2015;73:4–17. [PubMed: 25536338]
37. Madisen L, Mao T, Koch H, Zhuo J, Berenyi A, Fujisawa S, et al. A toolbox of Cre-dependent optogenetic transgenic mice for light-induced activation and silencing. Nat Neurosci. 2012;15:793–802. [PubMed: 22446880]
38. Madisen L, Garner AR, Shimaoka D, Chuong AS, Klapoetke NC, Li L, et al. Transgenic mice for intersectional targeting of neural sensors and effectors with high specificity and performance. Neuron. 2015;85:942–58. [PubMed: 25741722]
39. Harris JA, Hirokawa KE, Sorensen SA, Gu H, Mills M, Ng LL, et al. Anatomical characterization of Cre driver mice for neural circuit mapping and manipulation. Front. Neural Circuits. 2014;8: 76. [PubMed: 25071457]
40. Ramos RL, Van Dine SE, Gilbert ME, Leheste JR, Torres G. Neurodevelopmental malformations of the cerebellar vermis in genetically engineered rats. Cerebellum. 2015;14:624–31. [PubMed: 25700682]
41. Gong S, Doughty M, Harbaugh CR, Cummins A, Hatten ME, Heintz N, et al. Targeting Cre recombinase to specific neuron populations with bacterial artificial chromosome constructs. J Neurosci. 2007;27:9817–23. [PubMed: 17855595]
42. Schmidt EF, Kus L, Gong S, Heintz N. BAC Transgenic mice and the GENSAT database of engineered mouse strains. Cold Spring Harb Protoc 2013;2013(3). 10.1101/pdb.top073692.
43. Gerfen CR, Paletzki R, Heintz NGENSATBAC. Cre-recombinase driver lines to study the functional organization of cerebral cortical and basal ganglia circuits. Neuron. 2013;80:1368–83. [PubMed: 24360541]
44. Shima Y, Sugino K, Hempel CM, Shima M, Taneja P, Bullis JB, et al. A mammalian enhancer trap resource for discovering and manipulating neuronal cell types. elife. 2016;5:e13503. [PubMed: 26999799]
45. Laurie DJ, Wisden W, Seeburg PH. The distribution of thirteen GABAA receptor subunit mRNAs in the rat brain. III. Embryonic and postnatal development. J Neurosci. 1992;12:4151–72. [PubMed: 1331359]
46. Takayama C, Inoue Y. Morphological development and maturation of the GABAergic synapses in the mouse cerebellar granular layer. Brain Res Dev Brain Res. 2004;150:177–90. [PubMed: 15158081]
47. Graus-Porta D, Blaess S, Senften M, Littlewood-Evans A, Damsky C, Huang Z, et al. Beta1-class integrins regulate the development of laminae and folia in the cerebral and cerebellar cortex. Neuron. 2001;31:367–79. [PubMed: 11516395]
48. Li YN, Radner S, French MM, Pinzón-Duarte G, Daly GH, Burgeson RE, et al. The γ3 chain of laminin is widely but differentially expressed in murine basement membranes: expression and functional studies. Matrix Biol. 2012;31:120–34. [PubMed: 22222602]
49. Myshrall TD, Moore SA, Ostendorf AP, Satz JS, Kowalczyk T, Nguyen H, et al. Dystroglycan on radial glia end feet is required for pial basement membrane integrity and columnar organization of

the developing cerebral cortex. J Neuropathol Exp Neurol. 2012;71: 1047–63. [PubMed: 23147502]

50. Nguyen H, Ostendorf AP, Satz JS, Westra S, Ross-Barta SE, Campbell KP, et al. Glial scaffold required for cerebellar granule cell migration is dependent on dystroglycan function as a receptor for basement membrane proteins. Acta Neuropathol. Commun 2013;1:58. [PubMed: 24252195]
51. He M, Tucciarone J, Lee S, Nigro MJ, Kim Y, Levine JM, et al. Strategies and tools for combinatorial targeting of GABAergic neurons in mouse cerebral cortex. Neuron. 2016;91(6): 1228–43. [PubMed: 27618674]

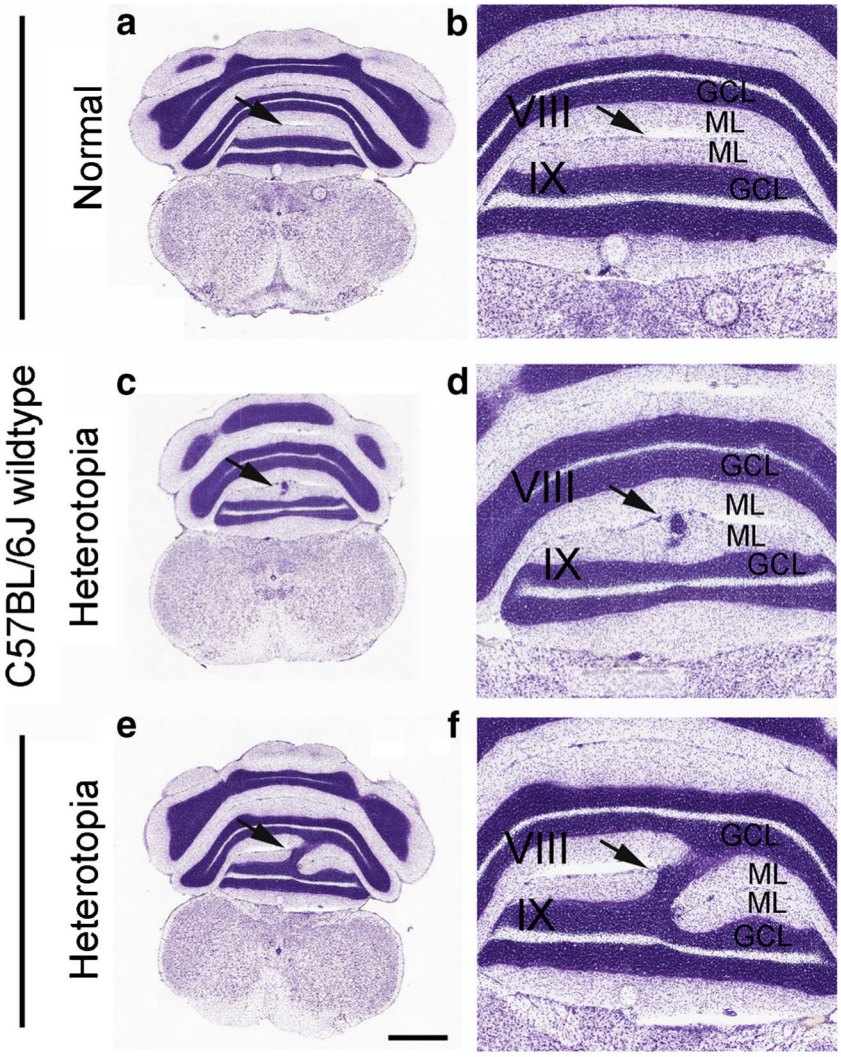

Fig. 1.

Nissl-stained, coronal sections of C57BL/6J mice demonstrating the normal (**a–b**) posterior vermis and 2 examples (**c–d** and **e–f**) of heterotopia from 2 different C57BL/6J mice (all data from Allen Brain Atlas). Scalebars in microns: a, c, e = 1049; b, d, f = 420

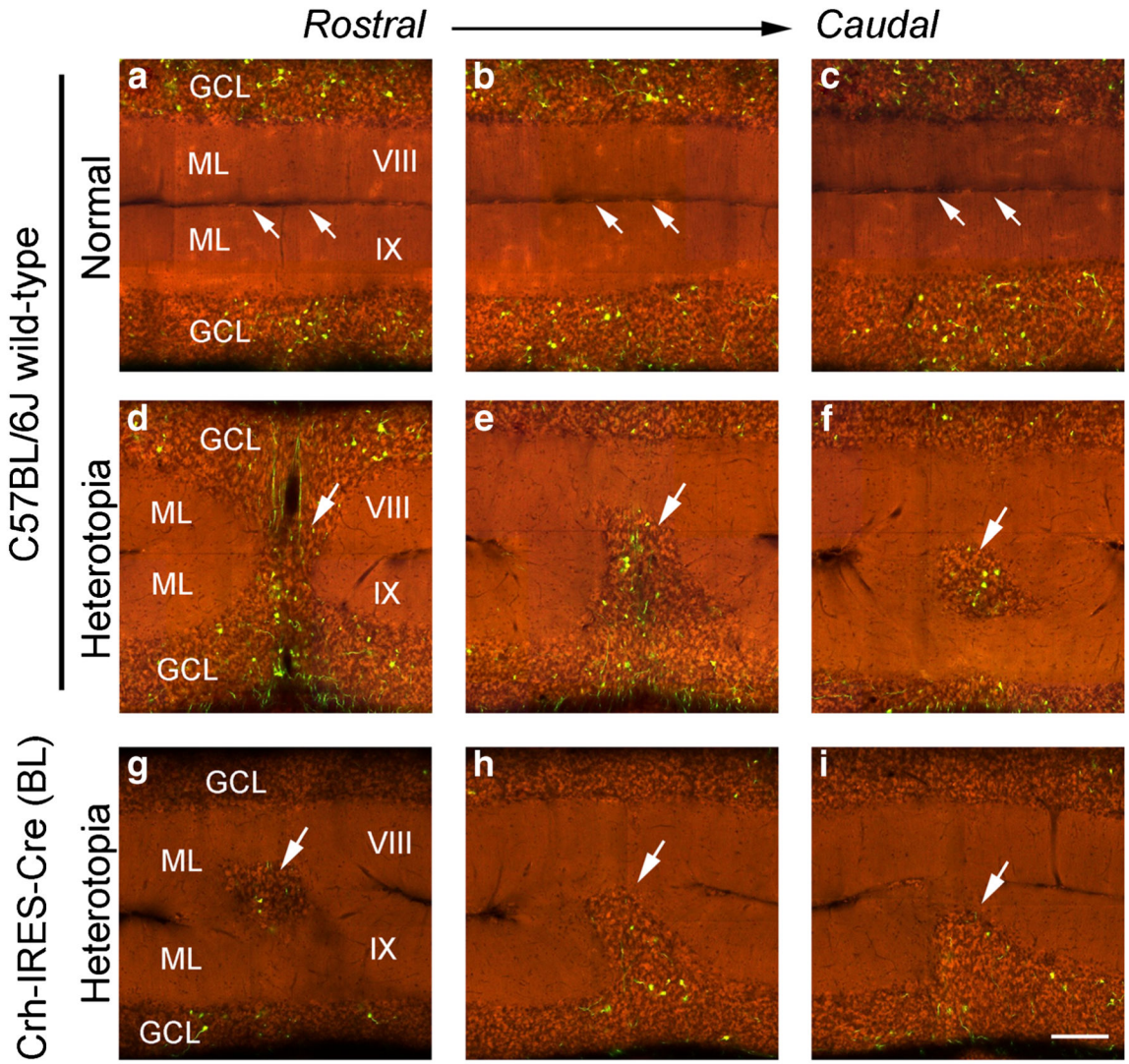

Fig. 2.

Serial, coronal sections demonstrating the normal (**a–c**) and malformed (d–f) organization of molecular layers between lobules VIII and IX in C57BL/6J mice. Note GFP-labeled mossy fibers in the granule cell layers as well as among heterotopic neurons (arrows in **d–f**). Serial, coronal sections demonstrating heterotopic neurons in the molecular layer of a Crh-IRES-Cre(BL) mouse (experiement:167213641) which was injected with a *Cre*-dependent virus targeting the dorsal cochlear nucleus. Note GFP-labeled mossy fibers in the granule cell layers as well as among heterotopic neurons. Refer to Table 1 for official names of GE mouse line used in this figure. All data from the *Mouse Connectivity Database* of the Allen Brain Atlas. Scalebars in microns: a–i = 140

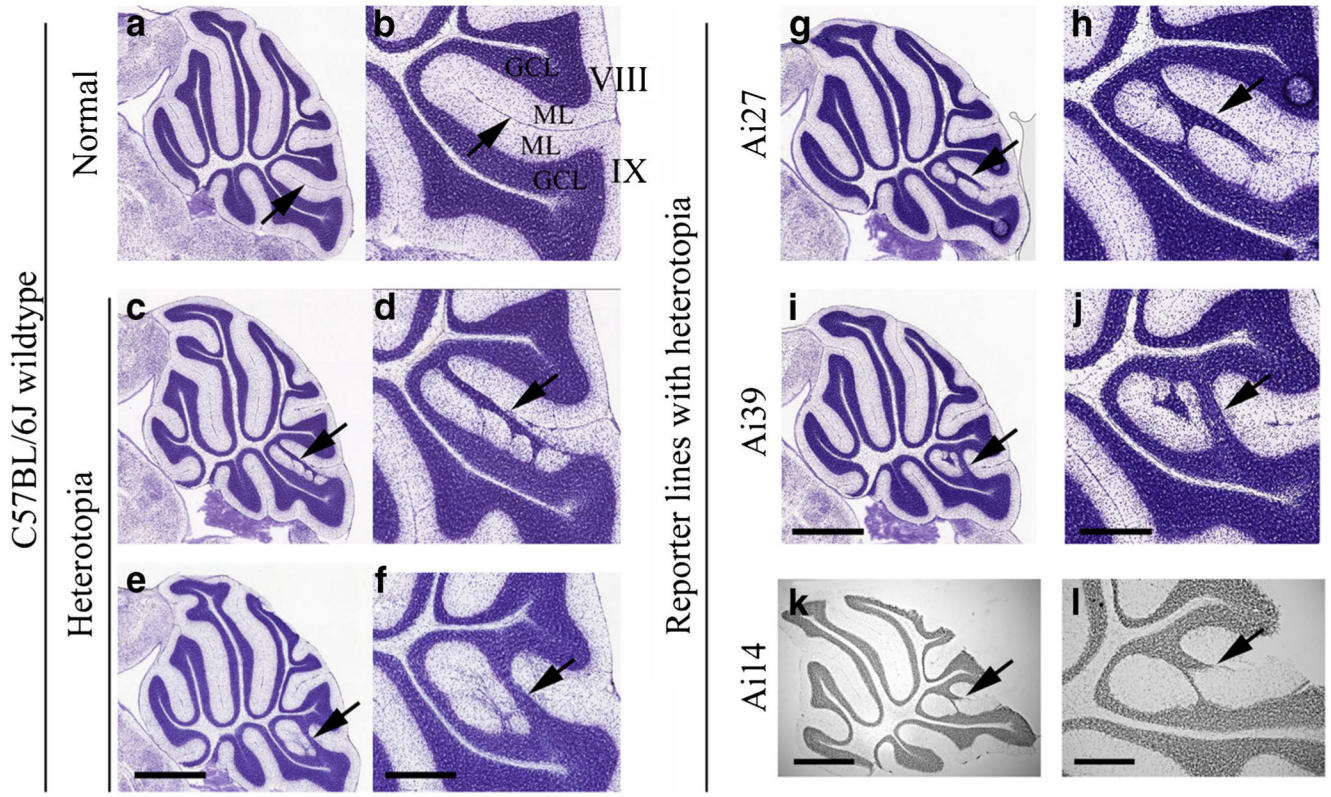

Fig. 3.

a–d Nissl-stained, sagittal sections of C57BL/6J mice demonstrating the normal posterior vermis (a) and two examples (c–d) of heterotopia from two different C57BL/6J mice. G-L, Nissl-stained, sagittal sections of three different reporter mouse lines demonstrating heterotopia of the posterior vermis. Refer to Table 1 for official names of GE mouse lines used in this figure. Data in **a–j** from the *Transgenic Characterization Database* of the Allen Brain Atlas. Scalebars in microns: a, c, e = 1199; b, c, f = 466; g, i = 1141; h, j = 399; k = 1000; l = 400

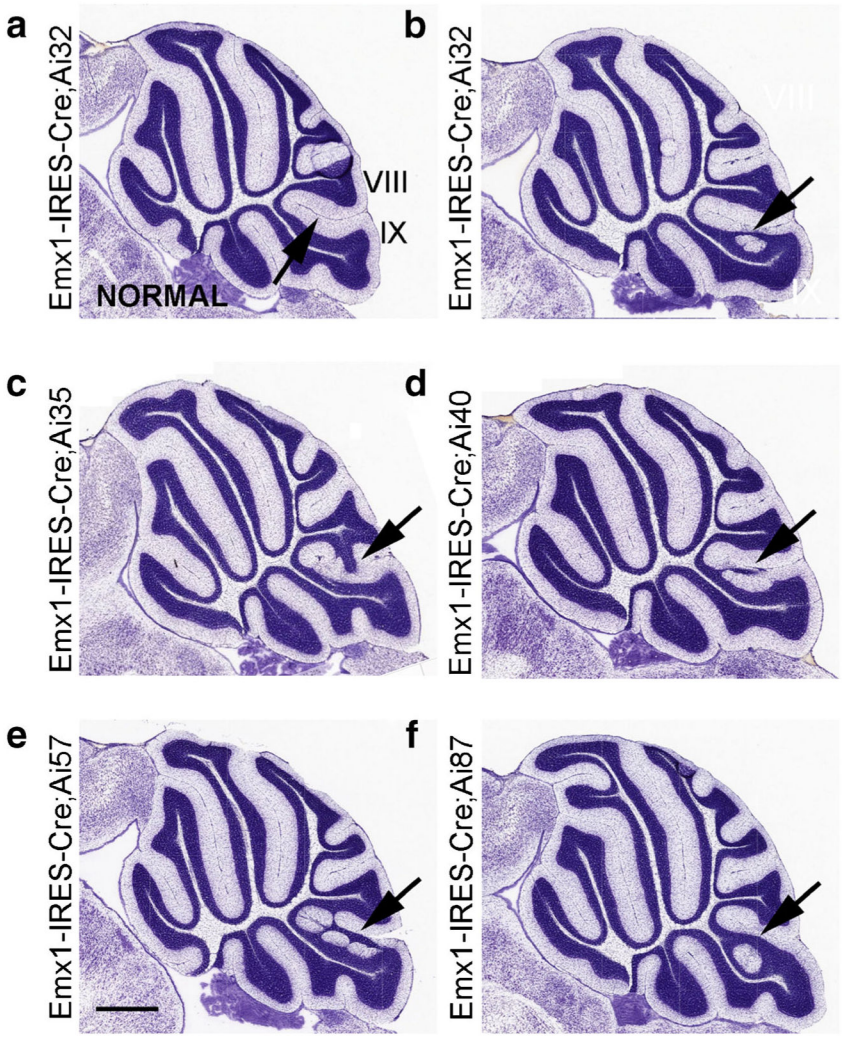

Fig. 4.

Nissl-stained, sagittal sections of different F1 hybrid mice demonstrating a normal posterior vermis (**a**) and examples of heterotopia (**b–f**) following crossing of Emx1-IRES-Cre mice with different reporter lines. Refer to Tables 1 and 2 for official names of GE mouse lines used in this figure. All data from the *Transgenic Characterization Database* of the Allen Brain Atlas. Scalebars in microns: a, b, f = 799; c = 879; d, e = 791

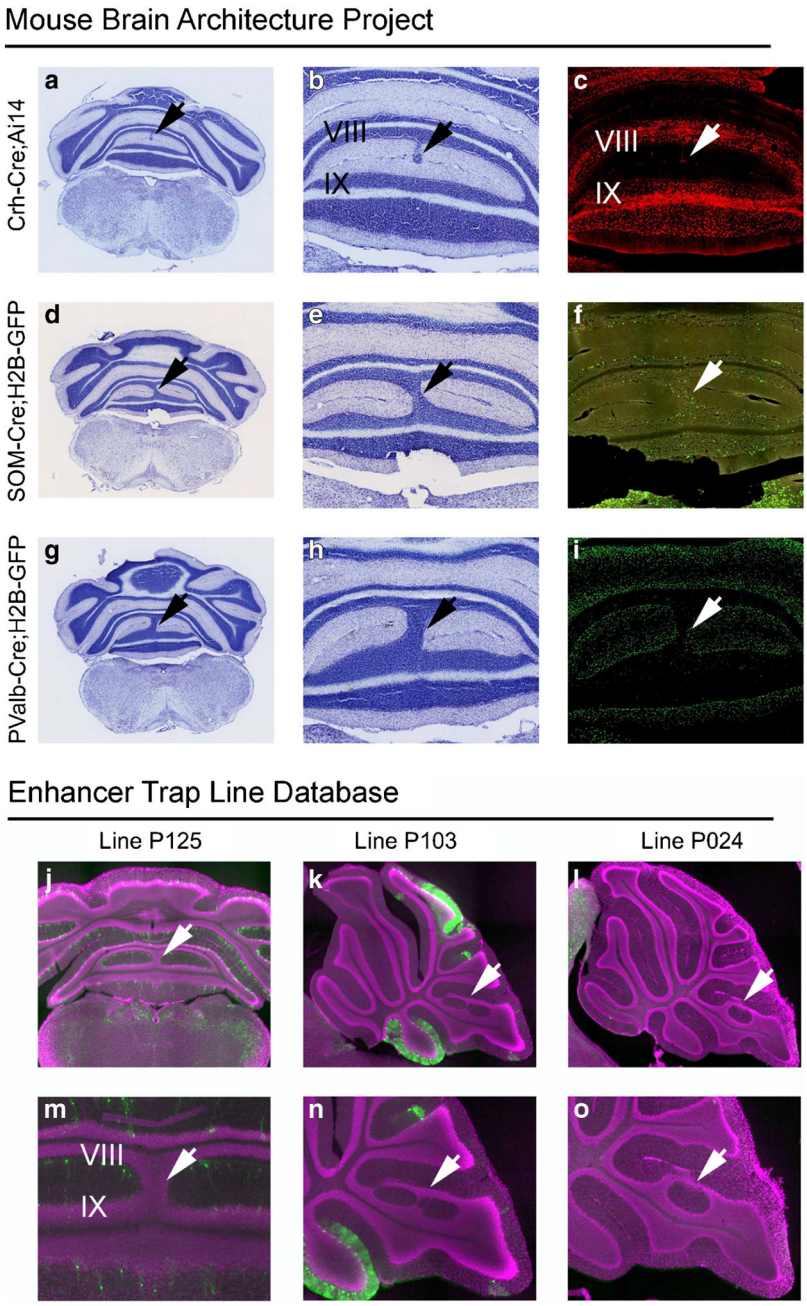

Fig. 5.

a–i Nissl staining (left and middle panels) and reporter protein expression (right panels) in adjacent sections from three different *Cre*-driver/*loxP* reporter F1 hybrid mice with heterotopia from the MBAP database. Refer to Table 3 for official names of mouse lines used in a–g. **j–o** Examples of three different GE mouse lines with heterotopia from the eTRAP database. Arrows in all panels point to heterotopia

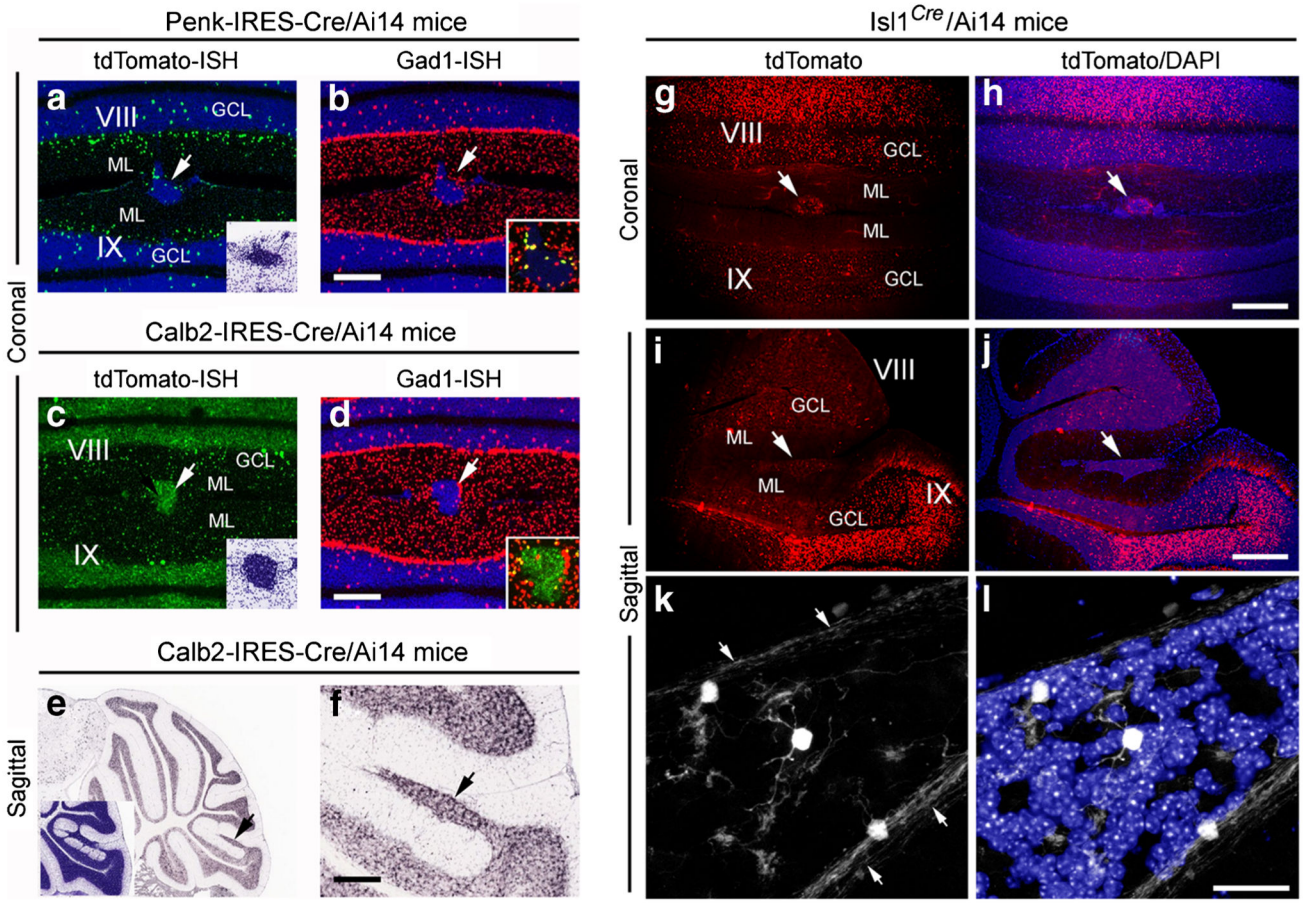

Fig. 6.

Coronal (**a–d**, **g–h**) and sagittal (**e–f**, **i–l**) of different *Cre*-driver lines crossed with *Ai14* reporter mice exhibiting heterotopia. tdTomato (a) and Gad1 (b) expression in a Penk-IRES-Cre;*Ai14* mouse indicates the presence of Penk-expressing GABAergic neurons in heterotopia. Inset in a is nissl staining of heterotopia in adjacent section from same mouse. tdTomato (a) and Gad1 (b) expression in a Calb2-IRES-Cre;*Ai14* mouse indicates the presence of granule cells and GABAergic neurons in heterotopia. Inset in c is nissl staining of heterotopia in adjacent section from same mouse. Sagittal sections (e–f) from another Calb2-IRES-Cre;*Ai14* mouse with numerous *Calb2*-granule cells in the heterotopia. Inset in e is nissl staining of heterotopia in adjacent section from same mouse. Refer to Table 1 for official names of mouse lines used in a–e. tdTomato fluorescence (i) and DAPI counterstaining (j) in a coronal section from a $Isl1^{Cre}$;*Ai14* mouse indicates the presence of granule neurons in heterotopia. tdTomato fluorescence (g) and DAPI counterstaining (h) in a sagittal section from a $Isl1^{Cre}$;*Ai14* mouse indicates the presence of granule neurons in heterotopia. k–l, High magnification of labeled granule cells and axons (arrows) from heterotopia in same brain. Refer to Table 1 for official names of mouse lines used in this figure. Data in a–f from the *Transgenic Characterization Database* of the Allen Brain Atlas. Scalebars in microns: a–d = 262; e = 879; f = 198; g–j = 300; k, l = 25

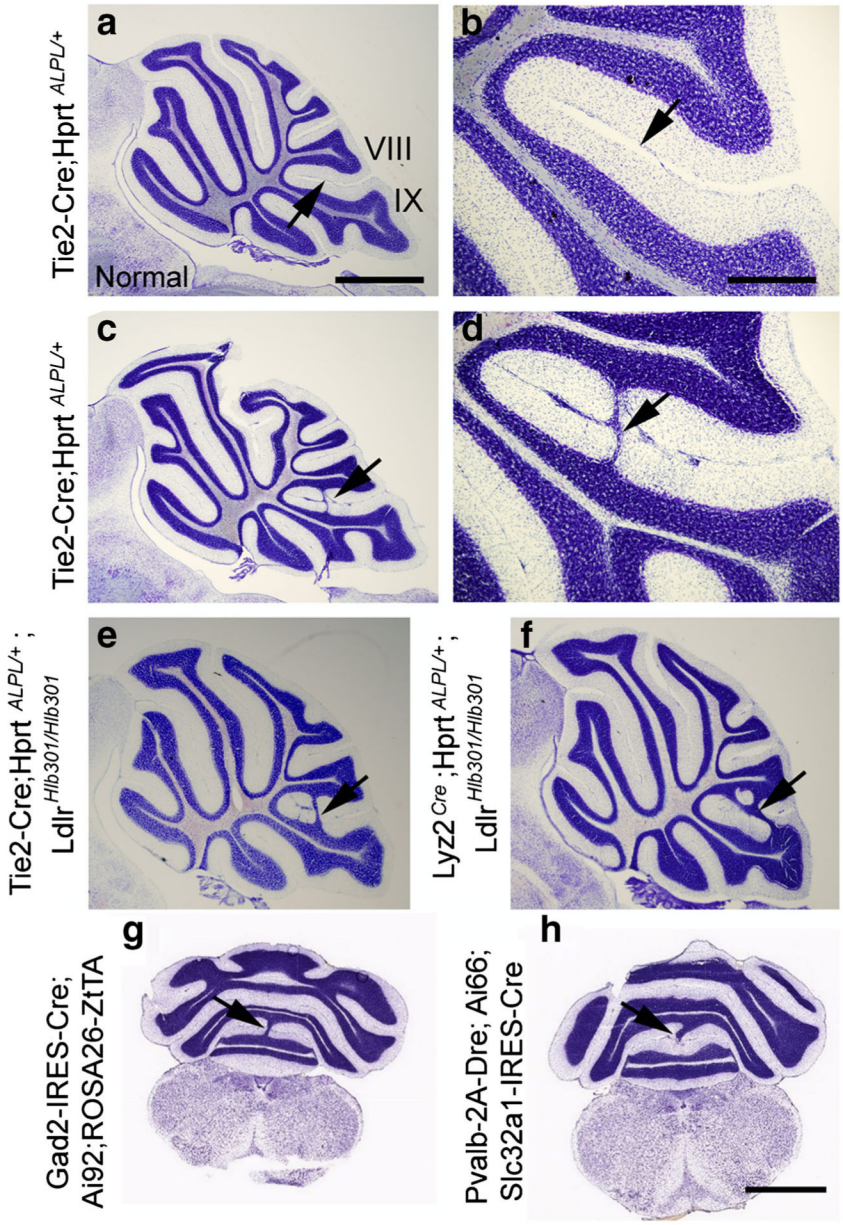

Fig. 7.

Nissl-stained sections from F1 mice from *Tie2-Cre or Lyz2*^{Cre} driver lines crossed to *Hprt*$^{ALPL/ALPL}$ reporter mice (**a–d**). Arrows point to normal molecular layer (**a–b**) or heterotopia in affected brains (**c–e**). Heterotopia in complex crosses consisting of three different lines (**e–h**). Data in gand h from the Allen Brain Atlas. Scalebars in microns: a, c, e, f = 1000; b, d = 400; g, h = 1756

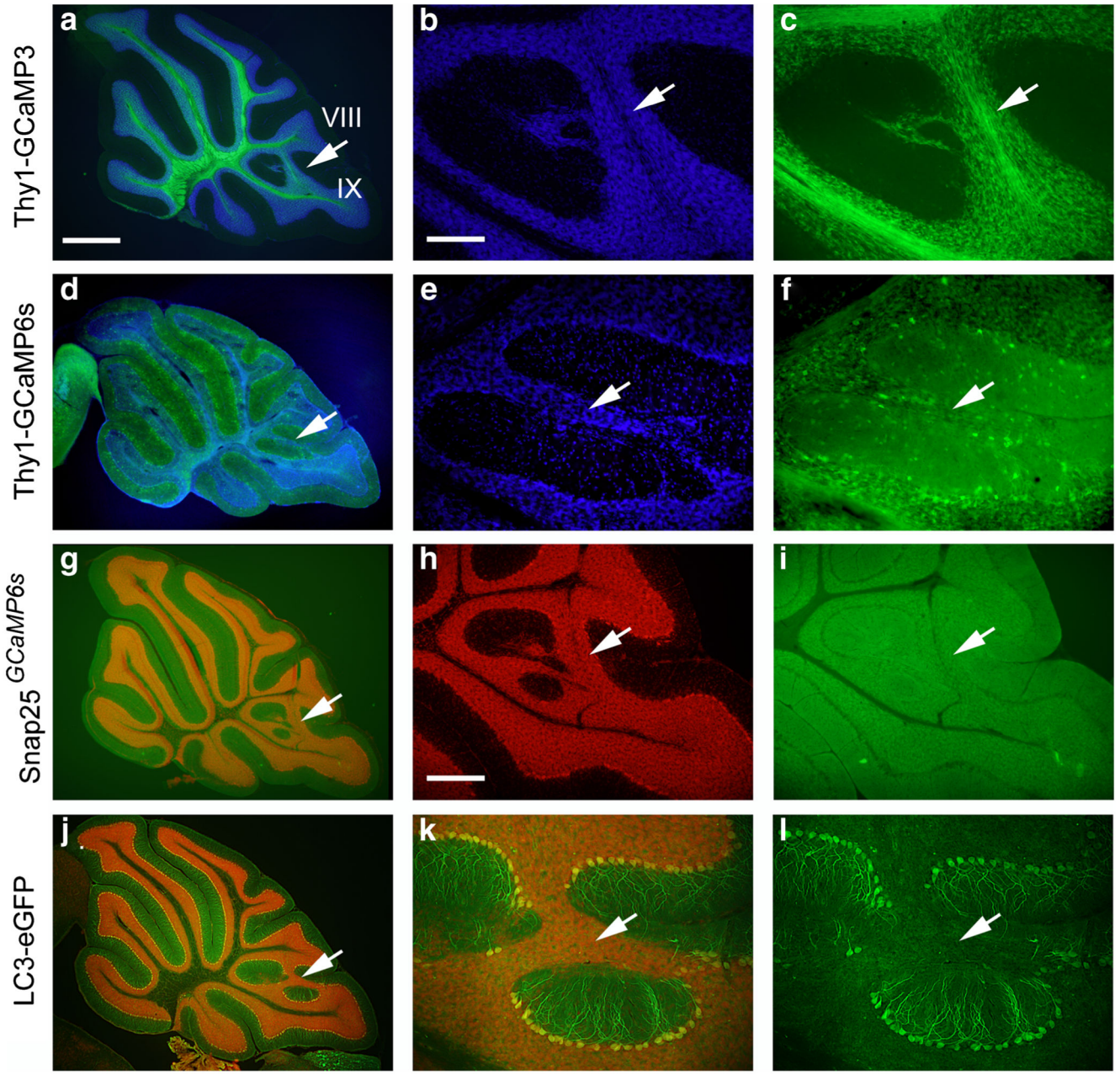

Fig. 8.

Sagittal sections from *Thy1-GCaMP3* (**a–c**), *Thy1-GCaMP6s* (**d–f**), *Snap25*^{GCaMP6s} (**g–i**), and *LC3-eGFP* (**j–l**) lines with heterotopia. Native GCaMP or GFP expression shown (green) as well as counterstaining with DAPI (blue) or propridium iodide (red) to demonstrate heterotopia. Low magnification images shown in left-side panels and higher magnification images of heterotopia shown in middle and right-side panels. Scalebars in microns: a, d, g, j = 750; b, c, e, f, k, l = 300; h, i = 150

Table 1

List of unique driver and reporter mouse lines exhibiting heterotopia as well as commercial vendor of each line (if available), number of brains examined for each line, percentage of affected brains, and experiment identification number of a representative example exhibiting heterotopia for evaluation in the ABA

Type	ABA driver line name	Source	Stock#	Background	Official mouse line nomenclature	N w/MLH	Total *N* examined	% w/MLH	Representative experiment w/MLH
Driver	A930038C07Rik-Tgl-Cre	Jax	17346	C57BL/6 congenic	B6.Cg-Tg(A930038C07Rik-cre)1Aibs/J	42	56	75.00	287461719
Driver	Adcyap1–2A-Cre	AIBS		C57BL/6 congenic	B6.Cg-*Adcyap1*$^{tm1.1(cre)Hze}$/ZakJ	8	11	72.73	303708513
Driver	Agrp-IRES-Cre	Jax	12899	C57BL/6 congenic	STOCK *Agrp*$^{tm1(cre)Lowl}$/J	2	3	66.67	167117360
Driver	Avp-IRES2-Cre	Jax	23530	C57BL/6 congenic	B6.Cg-*Avp*$^{tm1.1(cre)Hze}$/J	6	9	66.67	267398651
Driver	Calb1–2A-dgCre	Jax	23531	C57BL/6 congenic	B6.Cg-*Calb1*$^{tm1.1(folA/cre)Hze}$/J	1	1	100.00	293750063
Driver	Calb2-IRES-Cre	Jax	10774	C57BL/6 congenic	B6(Cg)-*Calb2*$^{tm1(cre)Zjh}$/J	20	33	60.61	168455487
Driver	Cart-Tg1-Cre	Jax	9615	C57BL/6 congenic	STOCK Tg(Cartpt-cre)1Aibs/J	9	15	60.00	176898557
Driver	Cck-IRES-Cre	Jax	12706	C57BL/6 congenic	STOCK *Cck*$^{tm1.1(cre)Zjh}$/J	8	9	88.89	159433187
Driver	Cdhr1-Cre_KG66	MMRRC	30952	C57BL/6 congenic	STOCK Tg(Cdhr1-cre)KG66Gsat/Mmucd	4	5	80.00	146921849
Driver	Chat-IRES-Cre	Jax	6410	C57BL/6 congenic	B6;129S6-*Chat*$^{tm2(cre)Lowl}$/J	14	26	53.85	177606140
Driver	Chrna2-Cre OE25	MMRRC	36502	C57BL/6 congenic	STOCK Tg(Chrna2-cre)OE25Gsat/Mmucd	5	42	11.90	304719312
Driver	Cnnm2-Cre KD18	MMRRC	30951	C57BL/6 congenic	STOCK Tg(Cnnm2-cre)KD18Gsat/Mmucd	2	4	50.00	167029528
Driver	Cort-T2A-Cre	Jax	10910	C57BL/6 congenic	STOCK *Cort*$^{tm1(cre)Zjh}$/J	5	5	100.00	157826227
Driver	Crh-IRES-Cre (BL)	Other		C57BL/6 congenic	Not reported	18	26	69.23	264707643
Driver	Crh-IRES-Cre (ZJH)	Jax	12704	C57BL/6 congenic	B6(Cg)-*Crh*$^{tm1(cre)Zjh}$/J	9	11	81.82	204832917
Driver	Cux2-CreERT2	MMRRC	32779	C57BL/6 congenic	B6(Cg)-*Cux2*$^{tm3.1(cre/ERT2)Mull}$/Mmmh	8	11	72.73	264873092
Driver	Cux2-IRES-Cre	MMRRC	31778	C57BL/6 congenic	B6(Cg)-*Cux2*$^{tm1.1(cre)Mull}$/Mmmh	48	65	73.85	278433737
Driver	Dbh-Cre_KH212	MMRRC	32081	C57BL/6 congenic	STOCK Tg(Dbh-cre)KH212Gsat/Mmucd	4	5	80.00	159942862
Driver	Drdla-Cre	Other		C57BL/6 congenic	Drd1$^{tm1(cre)Rpa}$	8	12	66.67	159942862
Driver	Drd2-Cre ER44	MMRRC	32108	C57BL/6 congenic	B6.FVB(Cg)-Tg(Drd2-cre)ER44Gsat/Mmucd	7	13	53.85	156670520
Driver	Drd3-Cre KI196	MMRRC	34610	C57BL/6 congenic	STOCK Tg(Drd3-cre)KI196Gsat/Mmucd	8	20	40.00	298759552
Driver	Drd3-Cre KI198	MMRRC	31741	C57BL/6 congenic	STOCK Tg(Drd3-cre)KI198Gsat/Mmucd	2	5	40.00	301122593
Driver	Efr3a-Cre_NO108	MMRRC	36660	C57BL/6 congenic	STOCK Tg(Efr3a-cre)NO108Gsat/Mmucd	2	41	4.88	301180385
Driver	Emxl-Ires-Cre	Jax	5628	C57BL/6 congenic	B6.129S2-*Emx1*$^{tm1(cre)Krj}$/J	8	17	47.06	478491090
Driver	Erbb4–2A-CreERT2	Jax	12360	C57BL/6 congenic	B6.Cg-*Erbb4*$^{tm1.1(cre/ERT2)Aibs}$/J	14	18	77.78	156742543
Driver	Esrl-2A-Cre	Other		C57BL/6 congenic	B6N.129S6(Cg)-*Esr1*$^{tm1.1(cre)And}$/J	1	7	14.29	264248605
Driver	Etvl-CreERT2	Jax	13048	C57BL/6 congenic	B6(Cg)-*Etv1*$^{tm1.1(cre/ERT2)Zjh}$/J	16	23	69.57	286772650

Type	ABA driver line name	Source	Stock#	Background	Official mouse line nomenclature	N w/MLH	Total *N* examined	% w/MLH	Representative experiment w/MLH
Driver	Gabra6-IRES-Cre	MMRRC	15968	C57BL/6 congenic	B6.129P2-*Gabra6*$^{tm2(cre)Wwis}$/Mmucd	1	3	33.33	159945113
Driver	Gabrr3-Cre KC112	MMRRC	30709	C57BL/6 congenic	STOCK Tg(Gabrr3-cre)KC112Gsat/Mmucd	1	8	12.50	170859382
Driver	Gad2-IRES-Cre	Jax	10802	C57BL/6 congenic	STOCK *Gad2*$^{tm2(cre)Zjh}$/J	39	64	60.94	299245589
Driver	Gal-Cre_KI87	MMRRC	31060	C57BL/6 congenic	STOCK Tg(Gal-cre)KI87Gsat/Mmucd	22	32	68.75	168002780
Driver	Glt25d2-Cre_NF107	MMRRC	36504	C57BL/6 congenic	STOCK Tg(Colgalt2-cre)NF107Gsat/Mmucd	1	4	25.00	506426038
Driver	Gng7-Cre_KH71	MMRRC	31181	C57BL/6 congenic	STOCK Tg(Gng7-cre)KH71Gsat/Mmucd	1	4	25.00	158017916
Driver	Gpr26-Cre_KO250	MMRRC	33032	C57BL/6 congenic	STOCK Tg(Gpr26-cre)KO250Gsat/Mmucd	14	31	45.16	301210923
Driver	Grik4-Cre	Jax	6474	C57BL/6 congenic	C57BL/6-Tg(Grik4-cre)G32–4Stl/J	14	28	50.00	177780284
Driver	Grm2-Cre_MR90	MMRRC	34611	FVB/N-Crl:CD(ICR)	STOCK Tg(Grm2-cre)MR90Gsat/Mmucd	5	27	18.52	264708349
Driver	Grp-Cre_KH288	MMRRC	31183	C57BL/6 congenic	STOCK Tg(Grp-cre)KH288Gsat/Mmucd	4	26	15.38	266583498
Driver	Hdc-Cre_IM1	MMRRC	32079	C57BL/6 congenic	STOCK Tg(Hdc-cre)IM1Gsat/Mmucd	2	4	50.00	168616827
Driver	Htr2a-Cre_KM207	MMRRC	31150	C57BL/6 congenic	STOCK Tg(Htr2a-cre)KM207Gsat/Mmucd	15	31	48.39	277957908
Driver	Htr3a-Cre_NO152	MMRRC	36680	C57BL/6 congenic	STOCK Tg(Htr3a-cre)NO152Gsat/Mmucd	5	10	50.00	305677409
Driver	Ins2-Cre	Jax	3573	C57BL/6 congenic	B6.Cg-Tg(Ins2-cre)25Mgn/J	2	5	40.00	265813096
Driver	Kcnc2-Cre	Jax	8582	C57BL/6 congenic	STOCK Tg(Kcnc2-Cre)K128Stl/LetJ	5	6	83.33	126853068
Driver	Kissl-Cre	Other		C57BL/6 congenic	STOCK Tg(Kiss1-cre)I2–4Cfe/J	1	4	25.00	232310521
Driver	Lepr-IRES-Cre	Jax	8320	C57BL/6 congenic	B6.129(Cg)-*Lepr*$^{tm2(cre)Rck}$/J	1	8	12.50	179904203
Driver	Lypd6-Cre_KL156	Other		Not reported	Not reported	1	11	9.09	298050269
Driver	Nosl-CreERT2	Jax	14541	C57BL/6 congenic	B6;129S-*Nos1*$^{tm1.1(cre/ERT2)Zjh}$/J	17	24	70.83	304997333
Driver	Nr5al-Cre	Jax	6364	C57BL/6 congenic	FVB-Tg(Nr5a1-cre)2Lowl/J	20	26	76.92	176882966
Driver	Ntrkl-IRES-Cre	MMRRC	15500	C57BL/6 congenic	B6;129S4-*Ntrk1*$^{tm1(cre)Ljr}$/Mmucd	17	27	62.96	262215150
Driver	Ntsrl-Cre_GN220	MMRRC	30648	C57BL/6 congenic	B6.FVB(Cg)-Tg(Ntsr1-cre)GN220Gsat/Mmucd	30	42	71.43	157768393
Driver	Nxph4–2A-CreERT2	Jax	22861	C57BL/6 congenic	B6.Cg-*Nxph4*$^{tm1.1(cre/ERT2)Hze}$/J	6	9	66.67	304612686
Driver	Otof-Cre	MMRRC	32781	C57BL/6 congenic	B6(Cg)-*Otof*$^{tm1.1(cre)Mul}$/Mmmh	1	3	33.33	182226133
Driver	Oxt-IRES-Cre	Other		C57BL/6 congenic	B6;129S-*Oxt*$^{tm1.1(cre)Dolsn}$/J	8	10	80.00	147051682
Driver	Oxtr-Cre_ON66	MMRRC	36545	FVB/N-Crl:CD(ICR)	STOCK Tg(Oxtr-cre)ON66Gsat/Mmucd	1	17	5.88	267762146
Driver	Pcdh9-Cre_NP276	MMRRC	36084	C57BL/6 congenic	STOCK Tg(Pcdh9-cre)NP276Gsat/Mmucd	2	8	25.00	267211671
Driver	Pcp2-Cre_GN135	MMRRC	30868	C57BL/6 congenic	B6.FVB(Cg)-Tg(Pcp2-cre)GN135Gsat/Mmucd	4	4	100.00	147708352
Driver	Pdzklipl-Cre_KD31	MMRRC	30851	C57BL/6 congenic	STOCK Tg(Pdzk1ip1-cre)KD31Gsat/Mmucd	12	16	75.00	167118084
Driver	Penk-IRES2-Cre	Jax	25112	C57BL/6 congenic	B6;129S-*Penk*$^{tm2(cre)Hze}$/J	1	2	50.00	306268688
Driver	Plxndl-Cre_OGl	MMRRC	36631	C57BL/6 congenic	STOCK Tg(Plxnd1-cre)OG1Gsat/Mmucd	6	13	46.15	293366741

Type	ABA driver line name	Source	Stock#	Background	Official mouse line nomenclature	N w/MLH	Total *N* examined	% w/MLH	Representative experiment w/MLH
Driver	Pmch-Cre	Jax	14099	C57BL/6 congenic	STOCK Tg(Pmch-cre)1Lowl/J	3	4	75.00	113506174
Driver	Pnmt-Cre	Other		C57BL/6 congenic	Pnmt$^{tm1(cre)Sne}$	2	4	50.00	156253662
Driver	Pomc-Cre (BL)	Jax	5965	C57BL/6 congenic	STOCK Tg(Pomc1-cre)16Lowl/J	3	4	75.00	159996191
Driver	Pomc-Cre (ST)	Jax	10714	C57BL/6 congenic	B6.FVB-Tg(Pomc-cre)1Lowl/J	2	3	66.67	113780276
Driver	Prkcd-GluCla-CFP-IRES-Cre	Other		C57BL/6 congenic	B6N.Cg-Tg(Prkcd-glc-1-rtTA)2And/J	12	17	70.59	278067445
Driver	Pvalb-IRES-Cre	Jax	8069	C57BL/6 congenic	B6;129P2-*Pvalb*$^{tm1(cre)Arbr}$/J	18	28	64.29	168401109
Driver	Rasgrf2–2A-dCre	Jax	22864	C57BL/6 congenic	B6;129S-*Rasgrf2*$^{tm1(cre/folA)Hze}$/J	5	13	38.46	313141786
Driver	Rbp4-Cre_KL100	MMRRC	31125	C57BL/6 congenic	STOCK Tg(Rbp4-cre)KL100Gsat/Mmucd	55	74	74.32	266250195
Driver	Rorb-IRES2-Cre	Jax	23526	C57BL/6 congenic	B6;129S-*Rorb*$^{tm1.1(cre)Hze}$/J	6	16	37.50	301580339
Driver	Scnnla-Tg2-Cre	Jax	9112	C57BL/6 congenic	B6;C3-Tg(Scnn1a-cre)2Aibs/J	13	14	92.86	162018879
Driver	Scnnla-Tg3-Cre	Jax	9613	C57BL/6 congenic	B6;C3-Tg(Scnn1a-cre)3Aibs/J	25	44	56.82	179640955
Driver	Siml-Cre	Jax	6451	C57BL/6 congenic	B6.FVB(129X1)-Tg(Sim1-cre)1Lowl/J	9	18	50.00	165035106
Driver	Siml-Cre_KJ18	MMRRC	31742	C57BL/6 congenic	STOCK Tg(Sim1-cre)KJ18Gsat/Mmucd	5	20	25.00	156195758
Driver	Slcl7a6-IRES-Cre	Other		C57BL/6 congenic	STOCK *Slc17a6*$^{tm2(cre)Lowl}$/J	38	52	73.08	181895006
Driver	Slcl7a7-IRES2-Cre	Jax	23527	C57BL/6 congenic	B6;129S-*Slc17a7*$^{tm1.1(cre)Hze}$/J	3	9	33.33	267106046
Driver	Slcl8a2-Cre_OZ14	MMRRC	34814	C57BL/6 congenic	STOCK Tg(Slc18a2-cre)OZ14Gsat/Mmucd	11	32	34.38	292958638
Driver	Slc32al-IRES-Cre	Other		C57BL/6 congenic	STOCK Slc32a1tm2(cre)Lowl/J	18	25	72.00	305320171
Driver	Slc6a3-Cre	Other		C57BL/6 congenic	Slc6a3$^{tm1(cre)Xz}$	4	10	40.00	166156241
Driver	Slc6a4-Cre_ET33	MMRRC	31028	C57BL/6 congenic	B6.FVB(Cg)-Tg(Slc6a4-cre)ET33Gsat/Mmucd	3	6	50.00	133286781
Driver	Slc6a4-CreERT2_EZ13	MMRRC	30071	C57BL/6 congenic	STOCK Tg(Slc6a4-cre/ERT2)EZ13Gsat/Mmucd	4	4	100.00	167212217
Driver	Slc6a5-Cre_KF109	MMRRC	30730	C57BL/6 congenic	STOCK Tg(Slc6a5-cre)KF109Gsat/Mmucd	10	15	66.67	157911126
Driver	Sst-IRES-Cre	Jax	13044	C57BL/6 congenic	STOCK *Sst*$^{tm2.1(cre)Zjh}$/J	10	19	52.63	304335875
Driver	Sytl7-Cre_NO14	MMRRC	34355	C57BL/6 congenic	STOCK Tg(Syt17-cre)NO14Gsat/Mmucd	16	26	61.54	299653551
Driver	Syt6-Cre_KI148	MMRRC	32012	C57BL/6 congenic	STOCK Tg(Syt6-cre)KI148Gsat/Mmucd	31	55	56.36	299820770
Driver	Tacl-IRES2-Cre	Jax	21877	C57BL/6 congenic	B6;129S-*Tac1*$^{tm1.1(cre)Hze}$/J	13	16	81.25	300843826
Driver	Tac2-IRES2-Cre	Jax	21878	C57BL/6 congenic	B6;129S-*Tac2*$^{tm1.1(cre)Hze}$/J	6	6	100.00	300927483
Driver	Th-Cre_FI172	MMRRC	31029	C57BL/6 congenic	B6.FVB(Cg)-Tg(Th-cre)FI172Gsat/Mmucd	10	14	71.43	304337288
Driver	Tlx3-Cre_PL56	MMRRC	36547	C57BL/6 congenic	STOCK Tg(Tlx3-cre)PL56Gsat/Mmucd	8	28	28.57	294533406
Driver	Trib2–2A-CreERT2	Jax	22865	C57BL/6 congenic	B6.Cg-*Trib2*$^{tm1.1(cre/ERT2)Hze}$/J	7	11	63.64	287601808
Driver	Ucn3-Cre_KF43	MMRRC	32078	C57BL/6 congenic	STOCK Tg(Ucn3-cre)KF43Gsat/Mmucd	2	4	50.00	127470976
Driver	Vip-IRES-Cre	Jax	10908	C57BL/6 congenic	STOCK *Vip*$^{tm1(cre)Zjh}$/J	9	10	90.00	182040934

Type	ABA driver line name	Source	Stock#	Background	Official mouse line nomenclature	N w/MLH	Total *N* examined	% w/MLH	Representative experiment w/MLH
Driver	Vipr2-Cre_KE2	MMRRC	34281	C57BL/6 congenic	STOCK Tg(Vipr2-cre)KE2Gsat/Mmucd	7	8	87.50	182805258
Driver	Wfel-Tg3-CreERT2	Jax	9103	C57BL/6 congenic	B6;C3-Tg(Wfs1-cre/ERT2)3Aibs/J	2	3	66.67	167793416
Driver	Chrnb4-Cre_OL57	MMRRC	36203	FVB/N-Crl:CDl(ICR)	STOCK Tg(Chrnb4-cre)OL57Gsat/Mmucd	0	7	0.00	
Driver	Fezfl-2A-dCre	Jax	25110	C57BL/6 congenic	B6.Cg-*Fezf1*$^{tm1.1(cre/folA)Hze}$/J	0	5	0.00	
Driver	Gnrhl-Cre	Other		Not reported	STOCK Tg(Gnrh1-cre)1Dlc/J	0	3	0.00	
Driver	Hcrt-Cre	Other		Not reported	Tg(HCRT-cre)1Stak	0	2	0.00	
Driver	Penk-2A-CreERT2	Jax	22862	C57BL/6 congenic	B6;129S-*Penk*$^{tm2(cre)Hze}$/J	0	1	0.00	
Driver	Ppplrl7-Cre_NL146	MMRRC	36205	FVB/N-Crl:CDl(ICR)	STOCK Tg(Ppp1r17-cre)NL146Gsat/Mmucd	0	40	0.00	
Driver	Satb2-Cre_MO23	MMRRC	32908	FVB/N-Crl:CDl(ICR)	STOCK Tg(Satb2-cre)MO23Gsat/Mmucd	0	4	0.00	
Driver	Sst-Cre	AIBS		Not reported	Not reported	0	1	0.00	
Driver	Th-IRES-CreER	Jax	8532	C57BL/6 congenic	B6;129- *Th*$^{tm1(cre/Esr1)Nat}$/J	0	1	0.00	
Driver	Wfsl-Tg2-CreERT2	Jax	9614	C57BL/6 congenic	B6.Cg-Tg(Wfs1-cre/ERT2)2Aibs/J	0	3	0.00	
Reporter	Ai27	Jax	12567	C57BL/6 congenic	B6.Cg-*Gt(ROSA)26Sor*$^{tm27.1(CAG-COP4*H134R/tdTomato)Hze}$/J	1	2	50.00	100144518
Reporter	Ai32	Jax	12569	C57BL/6 congenic	B6;129S-*Gt(ROSA)26Sor*$^{tm32(CAG-COP4*H134R/EYFP)Hze}$/J	1	2	50.00	100144597
Reporter	Ai39	Jax	14539	C57BL/6 congenic	B6;129S-*Gt(ROSA)26Sor*$^{tm39(CAG-hop/EYFP)Hze}$/J	1	2	50.00	100144578
Reporter	Ai75	Jax	25106	C57BL/6 congenic	B6.Cg-*Gt(ROSA)26Sor*$^{tm75.1(CAG-tdTomato*)Hze}$/J	9	20	45.00	528512680

Table 2

List of driver-reporter F1 hybrid mice exhibiting heterotopia and experiment identification number of a representative example exhibiting heterotopia for evaluation in the ABA. The stock number for purchase from The Jackson Laboratory is also indicated for each reporter line

ABA reporter line name	Reporter protein	Application	Official mouse line nomenclature	Jax stock#	Cre line crossed with (see Table 1)	Representative experiment
Ail4	tdTomato	Fluorescent visualization	B6;129S6-*Gt(ROSA)26Sor*$^{tm14(CAG-tdTomato)Hze}$/J	7914	Pvalb-IRES-Cre	81657984
Ai27	ChR2(H134R)-tdTomato	Fluorescent visualization/optical stimulation	B6.Cg-*Gt(ROSA)26Sor*$^{tm27.1(CAG-COP4*H134R/tdTomato)Hze}$/J	12567	Emx1-IRES-Cre	100144529
Ai3	EYFP	Fluorescent visualization	B6.Cg-*Gt(ROSA)26Sor*$^{tm3(CAG-EYFP)Hze}$/J	7903	Ntsrl-Cre GN220	81578128
Ai32	ChR2(H134R)-EYFP	Fluorescent visualization/optical stimulation	B6;129S-*Gt(ROSA)26Sor*$^{tm32(CAG-COP4*H134R/EYFP)Hze}$/J	12569	Emxl-IRES-Cre	100144601
Ai35	Arch-EGPP-ER2	Fluorescent visualization/optical inhibition	B6;129S-*Gt(ROSA)26Sor*$^{tm35.1(CAG-aop3/GFP)Hze}$/J	12735	Emxl-IRES-Cre	100132864
Ai39	eNpHR3.0-EGPP	Fluorescent visualization/optical inhibition	B6;129S-*Gt(ROSA)26Sor*$^{tm39(CAG-hop/EYFP)Hze}$/J	14539	Pvalb-IRES-Cre	100144576
Ai40	ArchT-EGPP	Fluorescent visualization/optical inhibition	B6.Cg-*Gt(ROSA)26Sor*$^{tm40.1(CAG-aop3/EGFP)Hze}$/J	21188	Emxl-IRES-Cre	100138935
Ai57	RCL-Jaws	Fluorescent visualization/optical inhibition	Not reported		Emxl-IRES-Cre	311807678
Ai62	tdTomato	Fluorescent visualization	B6.Cg-*Igs7*$^{tm62.1(tetO-tdTomato)Hze}$/J	22731	Camk2A-tTA	305620430
Ai75	tdTomato	Fluorescent visualization	B6.Cg-*Gt(ROSA)26Sor*$^{tm75.1(CAG-tdTomato*)Hze}$/J	25106	Snap25-IRES2-Cre	304699151
Ai87	iGluSnFR	Glutamate imaging	Not reported		Emxl-IRES-Cre	304699669
Ai9	tdTomato	Fluorescent visualization	B6.Cg-*Gt(ROSA)26Sor*$^{tm9(CAG-tdTomato)Hze}$/J	7909	Pvalb-2A-Cre	81657972
Ai92	YCX2.60	Calcium imaging	B6.Cg-*Igs7*$^{tm92.1(tetO-ECFP*/Venus*)Hze}$/J	12266	Gad2-IRES-Cre	313181852
Ai95	RCL-GCaMP6f	Calcium imaging	B6;129S-*Gt(ROSA)26Sor*$^{tm95.1(CAG-GCaMP6f)Hze}$/J	24105	Emxl-IRES-Cre	311807602
Snap25-LSL-2A-EGPP	EGPP	Fluorescent visualization	B6.Cg-*Snap25*$^{tm1.1Hze}$/J	21879	Trib2–2A-CreERT2	182271637

Table 3

List of *Cre*-driver mice and driver-reporter F1 hybrid mice exhibiting heterotopia in the MBAP databse. Experiment identification number of a representative example exhibiting heterotopia for evaluation in the MBAP database is also included. Note that all driver mice and *Ai14* mice are the same lines observed to have some prevalence of heterotopia in the ABA databases

MBAP Cre line	Official driver line nomenclature[a]	MBAP representative experiment	ABA representative experiment	MBAP reporter line	Reporter protein	Official reporter line nomenclature
Rbp4-Cre_KL100	STOCK Tg(Rbp4-cre)KL100Gsat/Mmucd	Ost4	266250195			
Ntsr1-Cre_GN220	B6.FVB(Cg)-Tg(Ntsr1-cre)GN220Gsat/Mmucd	Ost11	157768393			
Crh-IRES-Cre_ZJH	B6(Cg)-*Crh*$^{tm1(cre)Zjh}$/J	Hua108	156347602	Ail4[b]	tdTomato	B6.Cg-Gt(Rosa)26Sor$^{tm14(CAG-tdTomato)Hze}$/J
Pvalb-IRES-Cre	B6;129P2-*Pvalb*$^{tm1(cre)Arbr}$/J	Hual20	81657984	Ail4[b]	tdTomato	B6.Cg-Gt(Rosa)26Sor$^{tm14(CAG-tdTomato)Hze}$/J
Vip-IRES-Cre	STOCK *Vip*$^{tm1(cre)Zjh}$/J	Hual57	267224214	Ail4[b]	tdTomato	B6.Cg-Gt(Rosa)26Sor$^{tm14(CAG-tdTomato)Hze}$/J
Crh-IRES-Cre_ZJH	B6(Cg)-*Crh*$^{tm1(cre)Zjh}$/J	Hual82		H2B-GEP	GFP	B6;129S4-*Gt(ROSA)26Sor*$^{tm2(CAG-HIST1H2BB/EGFP)Zjh}$/J
Emx1-Ires-Cre	B6.129S2-Emx1tm1(cre)Krj/J	Hua57		H2B-GEP	GFP	B6;129S4-*Gt(ROSA)26Sor*$^{tm2(CAG-HIST1H2BB/EGFP)Zjh}$/J
Pvalb-IRES-Cre	B6;129P2-*Pvalb*$^{tm1(cre)Arbr}$/J	Hual54		H2B-GEP	GFP	B6;129S4-*Gt(ROSA)26Sor*$^{tm2(CAG-HIST1H2BB/EGFP)Zjh}$/J
Sst-IRES-Cre	STOCK Ssttm2.1(cre)Zjh/J	Hual41		H2B-GFP	GFP	B6;129S4-*Gt(ROSA)26Sor*$^{tm2(CAG-HIST1H2BB/EGFP)Zjh}$/J
Vip-IRES-Cre	STOCK Viptm1(cre)Zjh/J	Hual68		H2B-GFP	GFP	B6;129S4-*Gt(ROSA)26Sor*$^{tm2(CAG-HIST1H2BB/EGFP)Zjh}$/J

[a] Same as Table 1

[b] Same as Table 2